https://dx.doi.org/10.1016/j.trb.2019.07.016

Fleet Sizing for One-Way Electric Carsharing Services Considering Dynamic Vehicle Relocation and Nonlinear Charging Profile

Min Xu[a], *Qiang Meng*[b*]

[a] *Department of Industrial and Systems Engineering, The Hong Kong Polytechnic University, Hung Hom, Hong Kong*

[b] *Department of Civil and Environmental Engineering, National University of Singapore, Singapore 117576, Singapore*

Abstract

This study aims to determine the electric vehicle fleet size for one-way carsharing services by maximizing the profit of carsharing operators while taking into account the vehicle relocation operations and nonlinear electric vehicle charging profile. We formulate a set partitioning model for the considered problem. A tailored branch-and-price (B&P) approach is proposed to find the exact optimal solution of the model. In particular, an effective multi-label correcting method is developed to solve the pricing problem (i.e., generate columns) within the B&P approach. A novel non-dominated charging strategy is put up to avoid the exponential growth of labels caused by the allowance of partial charging with a nonlinear charging profile. In addition to the B&P approach, two heuristic methods are put forward for solving the large-scale problems or reinforcing the B&P approach. Numerical experiments with randomly generated instances and a case study based on a one-way carsharing operator in Singapore are conducted to further assess the efficiency and applicability of the proposed solution methods. The effects of several key parameters, i.e., the fixed cost of EV, relocation cost, electricity cost, service charge, EV driving range, the charging efficiency, and the number of rentals on the performance of a one-way electric carsharing system are also examined.

Keywords: one-way carsharing services, fleet size, electric vehicle, nonlinear charging profile, column generation, heuristics

1. Introduction

Carsharing is a flexible car-rental service that staggers the time of a group of users to drive a same car. As a prominent application of shared mobility, carsharing allows users to access mobility means without car ownership and has enjoyed a swift development over a few past years (Shaheen and Cohen, 2012; Weikl and Bogenberger, 2015). The traditional carsharing services require users to return cars to the original pick-up stations, which are referred to as the "two-way" carsharing services. To better serve the customers, some carsharing operators have switched to the "one-way" carsharing services that allow users to return the vehicles to any designated stations. Nevertheless, the convenience of the "one-way" carsharing services results in the vehicle imbalance issue across different stations, i.e., the number of vehicles/parking spots available at a specific station over a particular period is unable to accommodate user's demand. To tackle the vehicle imbalance issue, the costly dynamic vehicle relocation operations among parking stations are imperative for the carsharing operators (Boyacı et al., 2015; Nourinejad and Roorda, 2014; Nourinejad et al., 2015).

The advance of novel shared mobility has motivated many scholars from operations research to address the decision-making problems faced by carsharing operators either in a deterministic or stochastic environment (Benjaafar et al., 2017; Change et al., 2017; He et al., 2017; 2018; Lu et al., 2017; Nourinejad et al., 2015). Recently, the advent of electric vehicles (EVs) has made carsharing services more appealing to local governments by enabling sustainable development. With local governments in many countries offering various incentives to promote the adoption of EVs, more and more carsharing operators are expected to use EVs for their carsharing services. For example, the Land Transport Authority (LTA) and Economic Development Board (EDB) of Singapore have jointly launched the EV carsharing trial from 2014 to 2024 during which 1,000 EVs will be deployed in the one-way carsharing program to explore the viability of this innovative mobility in Singapore (LTA, 2014). Driven on electricity, however, EVs may create additional managerial problems in the one-way carsharing services due to their limited driving range per battery charge (Brandstätter et al., 2016, 2017; Illgen and Höck, 2018). The successful rental and relocation of EVs require that the vehicle should not get stagnant en route, and can be replenished when necessary by the charging facilities installed at parking spots at stations or along roads. The nonlinear charging profile, i.e., the state of charge (SOC) of EVs growing nonlinearly with respect to their charging time, has made the decision-makings more complicated (Pelletier et al. 2017). Therefore, the investigation into the challenging one-way electric-carsharing services considering the limited driving range and nonlinear charging profile of EVs is highly anticipated. This study aims to address a tactical planning problem in an electric carsharing system by determining the electric vehicle fleet size that maximizes the profit of a carsharing operator while taking the dynamic vehicle relocation and nonlinear charging profile of EVs into consideration. The considered problem is referred to as EVFS for short.

Constraining the range or time that an EV can travel in a day, especially in a situation where the EV can be replenished at home depots or public swapping/charging stations has been extensively examined in the context of shortest path problem and vehicle routing and/or scheduling problem (VRSP) (Adler and Mirchandani, 2016; Andelmin and Bartolini, 2017; Boysen et al., 2018; Desaulniers et al., 2016; Erdoğan and Miller-Hooks, 2012; Hiermann et al., 2016; Irnich and Desaulniers, 2005; Madankumar and Rajendran, 2018; Montoya et al., 2017; Pelletier et al., 2016; Schneider et al., 2014; Sweda et al., 2017; Toth and Vigo, 2002). The vehicle relocation problem of one-way carsharing services with a fleet of EVs has close parallel to VRSP with route or time constraints (VRSP-R/TC). As recently reviewed by Pelletier et al. (2017), however, all the relevant studies on the VRSP either assumed that EV should be charged to the fullest per battery charge with a fixed charging time penalty, or they allowed the partial charging but only with a simple linear or piece-wise linear approximation charging function. They emphasized the need to incorporate the nonlinear charging profile in the context of transportation problems with EVs.

A few studies have also been conducted for the decision-makings of one-way carsharing services while taking the charging requirement of EVs into account. For example, Li et al. (2016) optimized the station location and fleet size of an electric carsharing system using the continuum approximation approach. They assumed that EVs should be charged to the fullest before it can be picked up by the next user by adopting a linear or two-piece-wise linear charging profile. Bruglieri et al. (2014) formulated the vehicle relocation problem of one-way carsharing services with EVs as a paired pickup and delivery model with time windows. Bruglieri et al. (2017) later developed some heuristic methods for solving a similar model. Both studies allowed partial charging by assuming a linear charging profile. Boyaci et al. (2015) built a multi-objective mixed integer linear programming (MILP) model to address the strategic and tactical decisions considering vehicle relocation. Xu et al. (2018) developed a mixed-integer programming model and an effective global optimization method with several outer-approximation schemes to determine the optimal EV fleet size and trip price for one-way carsharing services. Both Boyaci et al. (2015) and Xu et al. (2018) mainly focused on the high-level decision-makings of EV carsharing services without paying attention to the detailed charging profile of EVs. Boyaci et al. (2017) later incorporated partial charging in an indirect manner for the investigation of the operational vehicle and personnel relocation problem of the one-way electric-carsharing services. With resorting to a simulation model, a trial-and-error method was proposed to assure that EVs would not run out of electricity when traveling on roads. Zhao et al. (2018) assumed a constant charging efficiency of EVs in their recent study of an integrated framework for EV rebalancing and staff relocation in one-way carsharing systems. A MILP model and a Lagrangian relaxation-based solution approach were developed to address the problem.

To the best of our knowledge, few studies have ever considered the nonlinear charging profile of EVs for the carsharing fleet sizing problem by using a discrete and exact optimization approach, although it is both practically relevant and important as pointed out by Pelletier et al. (2017). Assuming a full charge prohibits the utilization of EV especially in peak-hours and often results in an overestimation of the fleet size, while a linear charging profile overrates the charging efficiency and may lead to the underestimation of the fleet size. The discrepancy of the assumed charging function with respect to the realistic nonlinear charging profile reduces the credibility and quality of the solution. In this study, we will bridge the research gap by incorporating the nonlinear charging profile and the flexibility to allow partial charging in the fleet size determination for the one-way carsharing services with EVs. We assume that each EV has a limited driving range and parking spots are equipped with the charging facilities where EVs can be charged when parked. Our objective is to maximize the profit of a carsharing operator by determining the EV fleet size subject to the vehicle relocation and battery charging operations. To achieve this objective, a set partitioning model will be built for the considered problem. A tailored branch-and-price (B&P) approach is subsequently proposed to solve the model. The pricing problem embedded in the B&P approach to determine the relocation operation and charging strategy of an EV is different from the conventional minimum cost path problem of EVs in the manner that the EVs are charged partially by a nonlinear profile rather than be charged fully and instantly on arrival. If the column generation method for solving the pricing problem produces a non-integer optimal solution, a branch-and-bound method is used to repeatedly solve the pricing problem until an integer solution is found. The proposed B&P approach can yield the optimal EV fleet size for one-way carsharing services. In addition, two heuristic methods will be developed to effectively solve the large-scale problems or reinforce the B&P approach.

The remainder of this study is organized as follows. Assumptions, notations and the description of the EVFS problem are elaborated in Section 2. A set partitioning model for the EVFS problem is built in Section 3. The B&P approach for solving the model is developed in Section 4. Section 5 proposes two efficient heuristic methods to solve the large-scale instances or to reinforce the B&P approach. In addition, through the numerical experiments of randomly generated instances and a case study of SMOVE in Singapore, the efficiency of the proposed solution methods, and the effects of key parameters on the system performance of carsharing services are demonstrated in Section 6. Conclusions and future research directions are presented in Section 7.

2. Assumptions, Notations and Problem Description

Consider a carsharing operator who operates the daily one-way carsharing services using a fleet of homogenous EVs among a number of pre-determined stations located in an urban area. All these stations are grouped into a set denoted by $\mathcal{S}$. Each parking spot in the designated stations is equipped with a normal charging facility, and EVs can only be charged when parking at the designated stations[1]. The SOC of battery used by EVs grows nonlinearly with respect to the charging time. To explicitly elaborate the EVFS problem, the following subsections will cover several aspects including (i) the rentals, relocations and trip chains; (ii) feasibility, revenue and cost of a trip chain; (iii) the nonlinear charging profile of EVs; and (iv) the joint consideration of rental selection, vehicle relocation and charging strategy. The notations used throughout this study can be found in Appendix.

2.1. Rentals, Relocations and Trip Chains

All the rentals, i.e., carsharing service orders, requested from users are grouped into a set denoted by $\mathcal{I}$. The rental $i \in \mathcal{I}$ is described by a quintuple $U_i = \{s_i^o, s_i^d, t_i^o, t_i^d, e_i\}$, where $s_i^o \in \mathcal{S}$ represent the pick-up station, $s_i^d \in \mathcal{S}$ stands for the drop-off station, t_i^o denotes the departure time from the pick-up station, t_i^d indicates the arrival time at the drop-off station, and e_i is the amount of electricity consumed by the rental. Let G_i and OC_i denote the revenue collected from and the operating cost incurred by rental $i \in \mathcal{I}$, respectively. Note that

[1] This is current practice of some electric carsharing companies such as the BlueSG (https://www.bluesg.com.sg/). In order to avoid the detour to charge at other public stations, vehicles are required to be charged by the charging piles at the designated stations rather than the public charging stations. Note that this assumption is not restrictive because the modeling framework can be modified to consider charging at public stations as well.

the above information of rentals are assumed to be known a priori by estimation/prediction. This assumption is acceptable for tactical decision-making problem targeted by this study. How to estimate the demand for carsharing services is out of the scope of this study.

Vehicle relocation may be initiated from a station to another if there will be a customer setting out from that station without operationally available EVs by his/her departure time. Therefore an EV is generally relocated from the destination of a former user to the origin of the next customer. The EV relocation operation is characterized by its origin and destination stations. Assume that EVs would always travel on a pre-specified path (e.g., the shortest path) when relocated between two stations. Let $\tau(s_i^d, s_j^o)$ and $e(s_i^d, s_j^o)$ be the travel time and electricity consumption of that path from the drop-off station of rental $i \in \mathcal{I}$ to the pick-up station of rental $j \in \mathcal{I}$, respectively. The corresponding relocation cost is denoted by RC_{ij} . Note that s_i^d and s_j^o may represent the same physical stations, i.e., an EV is used for rental j right after rental i without relocation operation. Both $\tau(s_i^d, s_j^o)$ and $e(s_i^d, s_j^o)$ would be zero in this case.

The rental and relocation can be collectively referred to as "trip" since both of them are associated with an origin and a destination. An EV may be used by several users during the daily operation period, and vehicle relocations may be implemented between any two adjacent rentals to ensure that they are seamlessly connected. For ease of elaboration, we refer to the series of rentals and relocations underwent by an EV as a trip chain of that EV. Note that we do not consider users' choice behavior when picking up an EV among all vehicles in a station with heterogeneous SOC, and the definition of trip chain implies that customers would like to pick up any EV assigned by the operators for sake of system optimality. An EV trip chain r , which consists of a series of rentals sorted in an ascending order in terms of their departure times, i.e., $i_1, i_2, ..., i_{n_r}$, and several relocations linking these rentals, can be represented by

$$r = s_{i_1}^o \rightarrow s_{i_1}^d \Rightarrow s_{i_2}^o \rightarrow s_{i_2}^d \Rightarrow \cdots \Rightarrow s_{i_{n_r}}^o \rightarrow s_{i_{n_r}}^d \tag{1}$$

where the single and double lined arrows denote the rentals and relocations respectively. Suppose we have 6 rentals in a carsharing system with 7 stations. These rentals are numbered by 1, 2, 3, …, 6 in an ascending order of their departure times. Figure 1 illustrates an EV trip chain originating from Station 1 and returning back to the same station after going through 4 rentals (i.e., Rental 1,2,5,6) and 2 relocations (i.e., Station 3→2, 6→7). We can see that some rentals are connected directly without the EV relocation operation between them, and the EV relocation operation cannot be performed successively without a rental between them.

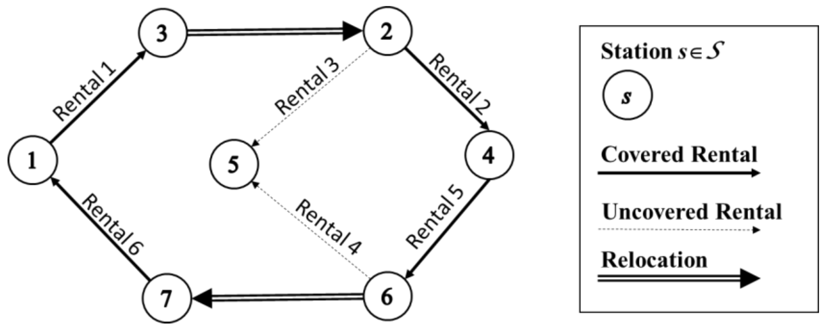

Figure 1. An example for the EV trip chain

2.2. Feasibility, Revenue and Operating Cost of an EV Trip Chain

An EV trip chain is feasible if it fulfills the two following conditions: (i) the relocation can be performed in time for the connection of next rental and (ii) the battery is sufficient to support all the trips given that EV can be charged at any passing stations if time permits. For example, for the trip chain r with rentals $i_1, i_2, ..., i_{n_r}$, the first condition can be asserted by the constraint:

$$\tau(s_{i_k}^d, s_{i_{k+1}}^o) \le t_{i_{k+1}}^o - t_{i_k}^d, \forall k = 1, 2, ..., n_r - 1 \tag{2}$$

For the ease of presentation, analogous to the expression of remaining electrical charge as SOC, the amount of electricity replenished at stations or consumed during trips are also expressed as the proportion of variation of electrical charge or discharge with respect to the maximum possible charge the battery can hold. Let $w(s_i^o)$ and $w(s_i^d)$ denote the amount of electricity charged at pick-up s_i^o and drop-off station s_i^d of rental i, respectively. For the trip chain with rentals $i_1, i_2, ..., i_{n_r}$, the SOC at the end of rental i_j is expressed by

$$SOC_{i_j} = SOC_{init} + \sum_{k=1}^{j-1}\left[w(s_{i_k}^o) + w(s_{i_k}^d) \right] + w(s_{i_j}^o) - \sum_{k=1}^{j} e_{i_k} - \sum_{k=1}^{j-1} e(s_{i_k}^d, s_{i_{k+1}}^o), \quad j = 1, 2, \cdots n_r \tag{3}$$

where SOC_{init} is the initial SOC of the EV at the very beginning of daily operation period.

The SOC right at the end of relocation operation from the drop-off station of rental i_j to the pick-up station of rental i_{j+1} is given by

$$SOC_{i_j,i_{j+1}} = SOC_{init} + \sum_{k=1}^{j}\left[w(s_{i_k}^o) + w(s_{i_k}^d) \right] - \sum_{k=1}^{j} e_{i_k} - \sum_{k=1}^{j} e(s_{i_k}^d, s_{i_{k+1}}^o),\ j = 1,2,...,n_r - 1 \tag{4}$$

Since the minimal SOC may occur either at the end of a rental or a relocation operation, in terms of electricity consumption, the second condition restricts that

$$SOC_{i_j} \geq SOC_{comf}, \forall j = 1,2,...,n_r \tag{5}$$

and

$$SOC_{i_j,i_{j+1}} \geq SOC_{comf}, \forall j = 1,2,...,n_r - 1 \tag{6}$$

where $SOC_{comf} \geq 0$ is the minimal comfortable SOC value that frees drivers from the range anxiety.

Let $\tau(s_i^o)$ and $\tau(s_i^d)$ denote the charging duration at the pick-up station s_i^o and drop-off station s_i^d of rental i, respectively. Hence in terms of charging time, the second condition limits that

$$\tau(s_{i_k}^d) + \tau(s_{i_{k+1}}^o) + \tau(s_{i_k}^d, s_{i_{k+1}}^o) \leq t_{i_{k+1}}^o - t_{i_k}^d, \forall k = 1,2,...,n_r - 1 \tag{7}$$

It can be seen that Eq. (2) readily follows from Eq. (7) given that $\tau(s_i^o)$ and $\tau(s_i^d)$ are all non-negative. Therefore, the feasibility of a trip chain consisting of rentals $i_1, i_2, ..., i_{n_r}$ only requires the constraints (5)-(7). In addition, except $w(s_{i_{n_r}}^d)$, the increment of $w(s_{i_j}^o)$ / $w(s_{i_j}^d)$ from SOC_{i_{j-1},i_j} / SOC_{i_j} with duration $\tau(s_{i_j}^o)/\tau(s_{i_j}^d)$ should align with the nonlinear charging profile of EVs, which will be elaborated in the next subsection.

The revenue of trip chain r is the sum of charge for the covered rentals, i.e., $R_r = \sum_{j=1}^{n_r} G_{i_j}$, while its operating cost consists of the fixed cost of an EV, which is denoted by EC and measured in \$/veh-day (e.g., the amortized cost, the depreciation cost, and the cost for insurance and maintenance, etc.), and the variable cost expressed by the sum of rental cost and relocation cost as follows:

$$E_r = \sum_{j=1}^{n_r} OC_{i_j} + \sum_{j=1}^{n_r - 1} RC_{i_j i_{j+1}} \tag{8}$$

2.3. Nonlinear Charging Profile

EVs can be charged at the designated stations after rentals or relocations, and the SOC grows nonlinearly with respect to the charging duration. The discharge of the battery of an EV occurs when the EV is traveling on road in the course of a rental or relocation. For simplicity, we assume that EVs travel in a speed without much variation such that the SOC would decrease linearly with travel distance/time until it reduces to the cut-off SOC value denoted by SOC_{cutoff}. This assumption is reasonable because it has been found that the discharging profile of battery is approximately linear if the EV travels in a constant or less vary speed (Larminie and Lowry, 2012; Pelletier et al., 2017).

The battery of an EV is generally charged with a constant current-constant voltage (CC-CV) or constant power-constant voltage (CP-CV) scheme (Liu, 2013). In both schemes the variation of battery's SOC cannot be assumed to be linear with respect the charging time, and the battery will not be deteriorated by overcharging under the realistic charging schemes (Pelletier et al., 2017). For ease of exposition, we assume without loss of generality that EVs are charged by the CC-CV scheme using the charging facilities in stations[2]. The CC-CV scheme suggests that in the charging process, a battery would first undergo the CC phase followed by the CV phase. In the CC phase, the charging current holds constant so that the SOC would increase linearly with time until the battery's terminal voltage reaches a threshold. After the CC phase, the charging process switches to the CV phase in which the terminal voltage holds constant, thus resulting in exponentially decreasing of charging current and concavely increasing of SOC (Marra et al., 2012).

We utilize the battery circuit model discussed by Pelletier et al. (2017) to describe the CC-CV charging scheme in which the variation of terminal voltage, charging current and SOC are monitored continuously. In particular, in the CC phase, let SOC_0 be the initial SOC before charging and I_{CC} be the constant charging current; then the SOC would increase linearly with charging duration as expressed by

$$SOC(t) = SOC_0 + \frac{I_{CC} \times t}{Cap} \tag{9}$$

[2] The model and solution methods are also applicable for charging with the CP-CV scheme.

where Cap denotes the maximum possible charge the battery can hold. The maximum SOC achieved at the end of CC phase is represented by $S\hat{O}C$. Let $\hat{t}$ denote the switch time point from CC phase to CV phase, after which SOC would vary according to a profile formulated by a complex differential equation. The maximum value of SOC achievable at the end of CV phase is denoted by SOC_{max}, and the duration of CV phase is represented by T_{max}. Figure 2 intuitively depicts the nonlinear charging profile by the CC-CV scheme from the cut-off SOC value to the maximum value SOC_{max}.

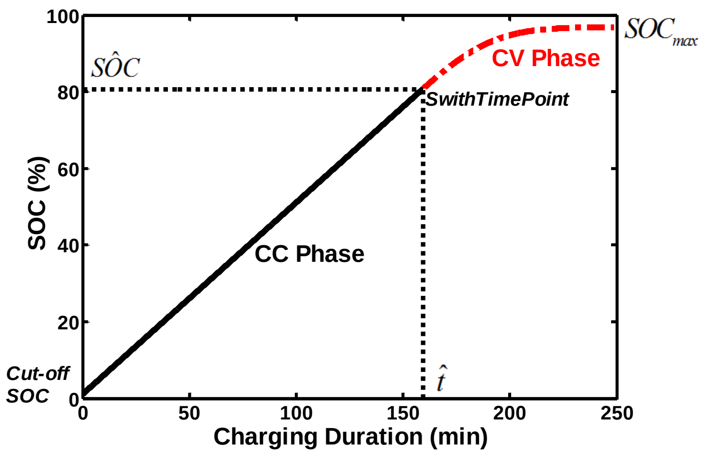

Figure 2. Illustration of nonlinear charging profile

Since the analytical expression of SOC in the CV phase does not exist, for ease of presentation, let $f(t)$ denote the implicit function of SOC with respect to time duration t in the CV phase, namely:

$$f(t) = SOC(t), t \in [0, T_{max}] \tag{10}$$

The inverse function of $f(t)$, denoted by f^{-1}, represents the function of charging time duration t with respect to the value of SOC, i.e., $t(SOC) = f^{-1}(SOC)$, where $SOC \in \left[S\hat{O}C, SOC_{max}\right]$. Given SOC_0, the final value of SOC after charging for t time duration under the CC-CV scheme is thus expressed by

$$FunSOC(SOC_0, t) = \begin{cases} SOC_0 + \frac{I_{CC} \times t}{Cap}, \text{if } \left(SOC_0 \le \hat{SOC}\right) \wedge \left(t \le \tau_1\right) \\ f(t - \tau_1), \quad \text{if } \left(SOC_0 \le \hat{SOC}\right) \wedge \left(\tau_1 < t < \tau_1 + T_{max}\right) \\ SOC_{max}, \quad \text{if } \left(SOC_0 \le \hat{SOC}\right) \wedge \left(t \ge \tau_1 + T_{max}\right) \\ f(t + \tau_2), \quad \text{if } \left(SOC_0 > \hat{SOC}\right) \wedge \left(t < T_{max} - \tau_2\right) \\ SOC_{max}, \quad \text{if } \left(SOC_0 > \hat{SOC}\right) \wedge \left(t \ge T_{max} - \tau_2\right) \end{cases} \tag{11}$$

where $\tau_1 = \frac{Cap \times (\hat{SOC} - SOC_0)}{I_{CC}}$ denotes the time required to charge from SOC_0 to the maximum SOC achieved at the end of CC phase, and $\tau_2 = f^{-1}(SOC_0)$ is the time required to charge from $\hat{SOC}$ to the initial value of SOC in the CV phase. Conversely, the time required to charge an EV from SOC_0 to $SOC_t \ge SOC_0$ is calculated by

$$FunTime(SOC_0, SOC_t) = \begin{cases} \frac{Cap \times (SOC_t - SOC_0)}{I_{CC}}, \text{if } SOC_t \le \hat{SOC} \\ \tau_1 + f^{-1}(SOC_t), \quad \text{if } \left(SOC_0 < \hat{SOC} < SOC_t\right) \\ f^{-1}(SOC_t) - \tau_2, \quad \text{if } SOC_0 \ge \hat{SOC} \end{cases} \tag{12}$$

2.4. Joint Consideration of Rental Selection, EV Relocation and EV Charging Strategy

For profit maximization, we assume that the carsharing operator allows the rejection of some rentals as long as it can boost the overall profit. The unserved rental i would incur a penalty denoted by P_i. The flexibility to allow partial charging entails the decision-making regarding the amount of electricity to be charged at each station. If less electricity is replenished at a station, the available electricity after charging may not be sufficient to sustain the next trip. However, if an EV stays longer to be charged for a larger amount of electricity, it may miss the departure time of the next trip. In addition, the nonlinear charging profile indicates distinct charging efficiency when initiating charging at different SOC, which means that the time required to replenish a certain amount of electricity may be different. The charging strategy, i.e., the charging amount/duration at each station, may be jointly considered along with the vehicle relocation operations when determining the EV fleet size for the one-way carsharing services.

As the vehicle relocation operations have been nicely reflected in EV trip chains, the objective of the EVFS problem is to maximize the daily profit of the carsharing operator by finding the optimal number of feasible trip chains in which EVs are relocated and charged appropriately and the selected rentals are satisfied successfully. There is no doubt that the proposed EVFS problem is NP-hard because the VRSP-R/TC as its special case without the requirement to charge vehicles has been demonstrated to be NP-hard by Ball (1980).

3. A Set Partitioning Model

Let $\mathcal{R}$ denote the set of all the feasible trip chains; then the proposed EVFS problem is formulated by the following set partitioning model:

$$\max_{x_r} \quad PROFIT = \sum_{r\in\mathcal{R}} (R_r - E_r - EC)x_r - \sum_{i\in\mathcal{I}} (1 - \sum_{r\in\mathcal{R}} \delta_r^i x_r) P_i \tag{13}$$

subject to

$$\sum_{r\in\mathcal{R}} \delta_r^i x_r \le 1, \quad \forall i \in \mathcal{I} \tag{14}$$

$$x_r \in \{0,1\}, \quad \forall r \in \mathcal{R} \tag{15}$$

where $x_r, r \in \mathcal{R}$ is the binary decision variable, $x_r = 1$ if trip chain $r \in \mathcal{R}$ is performed by an EV in the fleet; δ_r^i is the rental-trip chain incidence coefficient that equals 1 if rental i is covered by trip chain r, and 0 otherwise. The objective function expressed by Eq. (13) is the daily profit of a carsharing operator. Constraint (14) ensures that a rental is covered by at most one trip chain. Constraint (15) defines x_r as a binary variable. The integer programming model (13)-(15) can be equivalently expressed by

[EVFS]

$$\max_{x_r} \quad PROFIT^{new} = \sum_{r\in\mathcal{R}} (R_r - E_r - EC + \sum_{i\in\mathcal{I}} \delta_r^i P_i) x_r \tag{16}$$

subject to constraints (14)-(15).

The huge number of feasible trip chains makes the model [EVFS] intractable even for a small size problem. However, it could be solved by a well-designed branch-and-price approach as what Barnhart et al. (1998) pointed out. In case the B&P method is computationally intractable for large-scale problems, some reinforcements and heuristic methods may help to find an approximate solution in acceptable computational time.

4. Branch-and-Price Approach

The linear programming relaxation of model [EVFS], referred to as master problem (MP), can be solved through a column generation method by repeatedly solving a restricted master problem (RMP) with a subset of trip chains $\bar{\mathcal{R}} \subset \mathcal{R}$, and a pricing problem to find additional trip chains with positive reduced cost (for maximization problem). In case that the solution to the MP is not integer, a branch-and-bound (B&B) scheme should be adopted to obtain an integer solution. The B&P approach is a combination of column generation and B&B scheme, and its efficiency depends on how to effectively solve the pricing problem, i.e., generate columns, by exploring the unique problem features.

4.1. Pricing Problem

Let $\pi_i, \forall i \in \mathcal{I}$ denote the dual variable corresponding to constraint (14). The pricing problem for the MP of the model [EVFS], named by [EVFS-PP], is presented as follows:

[EVFS-PP]

$$P = \max_{r \in \mathcal{R} \setminus \bar{\mathcal{R}}} \quad R_r - E_r - EC + \sum_{i \in \mathcal{I}} \delta_r^i P_i - \sum_{i \in \mathcal{I}} \delta_r^i \pi_i \tag{17}$$

where the objective function expresses the reduced cost of the trip chains in the set $\mathcal{R} \setminus \bar{\mathcal{R}}$.

The problem [EVFS-PP] is to find the most profitable trip chain with an additional revenue $(P_i - \pi_i)$ from each covered rental among the rest trip chains. It can be formulated as the EV shortest path problem with nonlinear & partial replenishment, referred to as EVSPP-N&PR for short. The EV shortest path problem is significantly different from the conventional shortest path problem for gasoline vehicle because it allows loops in the optimal path due to the detours for charging. In addition, the existence of nonlinear & partial replenishment further requires a customized method to find the shortest path of EV. We now develop a multi-label method for solving the EVSPP-N&PR on a network constructed based on the rentals. The network construction needs several efficient pre-processes to eliminate those infeasible relocations and rentals in terms of time and/or electricity consumption.

4.1.1. Network construction procedure

We construct a pseudo-network denoted by $\mathcal{G} = (\mathcal{I}, \mathcal{A})$ to solve the EVSPP-N&PR. Any rental i is represented by a node $i \in \mathcal{I}$ in the network associated with the node cost $c_i = -(G_i - OC_i + P_i - \pi_i)$ and the electricity consumption e_i. The relocation operation from the drop-off station of rental i to the pick-up station of rental j is represented by a directed link $ij \in \mathcal{A} \subseteq \mathcal{I} \times \mathcal{I}$ from node i to node j associated with link cost $c_{ij} = RC_{ij}$. Each path in the constructed network is an EV trip chain, and the charging strategy at the drop-off station of a rental and the pick-up station of its adjacent next rental is implicitly implied in the directed link between the two rentals. The objective to find the trip chain with the largest profit is thus equivalent to finding the shortest path of EV in the constructed network $\mathcal{G}$. Figure 3 illustrates the network constructed for the pricing problem with the rentals in Figure 1.

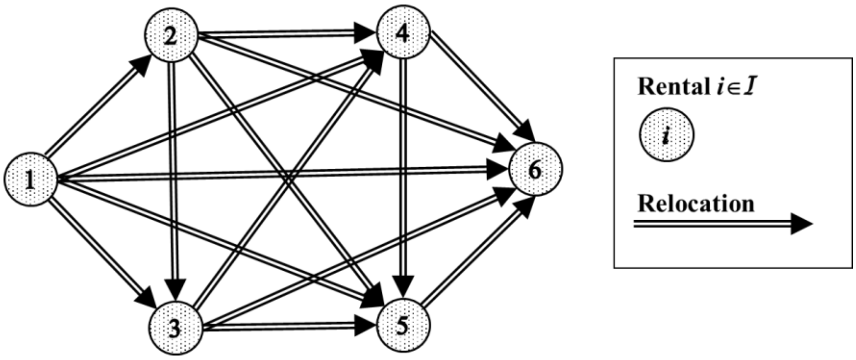

Figure 3. A constructed network

To eliminate the infeasible and un-optimal nodes and links, the above constructed network should be pre-processed. In view of the rental feasibility, any node with its electricity consumption exceeding $SOC_{max} - SOC_{min}$ where $SOC_{min} = \max\{SOC_{comf}, SOC_{cutoff}\}$, is removed from the constructed network, and the corresponding links are removed accordingly. For the link feasibility in terms of travel time and electricity consumption, any link ij can be excluded if either of the two conditions, $\tau(s_i^d, s_j^o) \le t_j^o - t_i^d$ and $e(s_i^d, s_j^o) \le SOC_{max} - SOC_{min}$, are not satisfied. To reduce model parameter, in practice we can normalize SOC_{min} to 0 and adjust all the other values of SOC accordingly. To sum up, the network construction procedure works as follows:

Step 1: Sort rentals in ascending order in terms of the departure time and name them in sequence as rental 1, rental 2, …, until rental $|\mathcal{I}|$.

Step 2: Check the feasibility of each rental and remove the infeasible rentals.

Step 3: For each remaining rental i and rental $j > i$, generate the directed link ij if both the following two conditions hold:

$$\tau(s_i^d, s_j^o) \le t_j^o - t_i^d \quad (18)$$

$$e(s_i^d, s_j^o) \le SOC_{max} - SOC_{min} \quad (19)$$

It should be pointed out that the network construction procedure does not consider the impact of charging strategy and nonlinear charging profile. In fact, a link with its tail and head is a special trip chain. According to the feasibility conditions of a trip chain in Subsection 2.2, the above feasibility check of links can be reinforced by two tighter conditions:

Condition 1: The total charging time at stations s_i^d and s_j^o should not exceed the difference of the elapsed time and travel time between rental i and rental j, namely:

$$\tau(s_i^d) + \tau(s_j^o) \le (t_j^o - t_i^d) - \tau(s_i^d, s_j^o) \quad (20)$$

Condition 2: An EV should at least be able to reach the pick-up and drop-off stations of rental j if it departs from the pick-up station of rental i with the maximum achievable SOC, i.e., SOC_{max}, considering the limitation of total charging time exposed in ***Condition 1*** and the nonlinear charging profile of battery described in Subsection 2.3. In other words, we have the following two requirements:

$$SOC_{i,j} = SOC_{max} - e_i + w(s_i^d) - e(s_i^d, s_j^o) \ge SOC_{min} \quad (21)$$

and

$$SOC_j = SOC_{max} - e_i + w(s_i^d) - e(s_i^d, s_j^o) + w(s_j^o) - e_j \ge SOC_{min} \quad (22)$$

where the increment of $w(s_i^d)$ / $w(s_j^o)$ from $(SOC_{max} - e_i)$ / $\left[SOC_{max} - e_i + w(s_i^d) - e(s_i^d, s_j^o)\right]$ with duration $\tau(s_i^d) / \tau(s_j^o)$ should align with the nonlinear charging profile. This implies that the following two equations must hold:

$$w(s_i^d) = FunSOC(SOC_{max} - e_i, \tau(s_i^d)) - (SOC_{max} - e_i) \quad (23)$$

$$\begin{aligned} w(s_j^o) = {} & FunSOC([SOC_{max} - e_i + w(s_i^d) - e(s_i^d, s_j^o)], \tau(s_j^o)) \\ & - [SOC_{max} - e_i + w(s_i^d) - e(s_i^d, s_j^o)] \end{aligned} \quad (24)$$

Any link ij violating either of the above two conditions should be excluded from the constructed network. The reinforced pre-processing procedure could significantly reduce the size of the network. It can be seen that the feasibility check of link ij is equivalent to examining the existence of nonnegative $\tau(s_i^d)$, $\tau(s_j^o)$, $w(s_i^d)$ and $w(s_j^o)$ such that Eqs. (20)-(24) hold. Although the pre-processing procedure can be reinforced by the two new conditions in principle, how to quantitatively validate the conditions can only be made clear after the non-dominated charging strategy is introduced.

4.1.2. Non-dominated charging strategy

The EVSPP-N&PR is an extension of the resource constrained shortest path problem by allowing detours and replenishments along a path. The replenishment opportunities entails multiple labels at each node in the network for solving the EVSPP-N&PR. A label at a node represents a path from an origin to that node, and is expressed by a two-dimensional vector: (the total cost of the path, final SOC of the path). Laporte and Pascoal (2011) have developed a multi-label method for solving the minimum cost path problem with relays (MCPPR), a special case of the EVSPP-N&PR with positive link costs and full & instant replenishments. According to Theorem 1 in Laporte and Pascoal (2011), one of the optimal solutions to the EVSPP-N&PR can be found by only retaining and updating the labels associated with non-dominated pairs of values of cost and SOC at each node.

Since the EVSPP-N&PR extends the MCPPR by allowing partial and nonlinear charging, a path in the EVSPP-N&PR includes additional information of the charging activities at the traversed stations. Those charging activities entail the following definitions of link and path charging strategy:

Definition 1: The charging strategy of a link ij refers to the charging amount and charging duration at the drop-off station of rental i and the pick-up station of rental j.

Definition 2: The charging strategy of a path refers to the charging strategies of all the traversed links.

The charging strategies for the individual links along a path are mutually independent except that the value of SOC after performing the charging strategy for a preceding link (minus the amount of electricity consumed at the head of the link) should be consistent with the SOC before performing the charging strategy for a subsequent link. A charging strategy is deemed as feasible if it ensures the feasibility of a link or path, and a link or path is feasible if there exists at least one feasible charging strategy.

The allowance of partial charging leads to a huge number of feasible charging strategies for a path. This creates problems when directly applying the multi-label method because they would result in the exponential growth of labels. We observe that the charging strategy only affects the value of SOC, and there always exists a non-dominated charging strategy for a link ij, by which the SOC at the departure time clock of rental j is no less than that by implementing any other feasible charging strategies. Hence, we may only need to generate labels at each node corresponding to the non-dominated charging strategy in solving the EVSPP-N&PR. The above finding suggests the following definition for the non-dominated charging strategy of a link:

Definition 3: A charging strategy for a link ij is non-dominated if the resultant SOC at the departure time of rental j is no less than that by any other feasible charging strategies.

For any link ij, let $SOC_j^o(SOC_i, m_{ij})$ denote the SOC at the departure time clock of rental j after setting off from the drop-off station of rental i at SOC_i and being charged by a charging strategy m_{ij} described by a quadruplet, i.e., $m_{ij} = \left\{\tau(s_i^d), \tau(s_j^o), w(s_i^d), w(s_j^o)\right\}$. All the feasible charging strategies for link ij are grouped into a set M_{ij}. According to Definition 3, a non-dominated charging strategy of link ij, denoted by $m_{ij}^* = \left\{\tau^*(s_i^d), \tau^*(s_j^o), w^*(s_i^d), w^*(s_j^o)\right\}$, can theoretically be found by solving the following optimization problem:

[NDCS $_{ij}$]

$$\max_{m_{ij} \in M_{ij}} SOC_j^o(SOC_i, m_{ij}) = SOC_i + w(s_i^d) - e(s_i^d, s_j^o) + w(s_j^o) \tag{25}$$

$$\tau(s_i^d) + \tau(s_j^o) \le (t_j^o - t_i^d) - \tau(s_i^d, s_j^o) \tag{26}$$

$$SOC_i + w(s_i^d) - e(s_i^d, s_j^o) \ge SOC_{min} \tag{27}$$

where

$$w(s_i^d) = FunSOC(SOC_i, \tau(s_i^d)) - SOC_i \tag{28}$$

$$w(s_j^o) = FunSOC(SOC_i + w(s_i^d) - e(s_i^d, s_j^o), \tau(s_j^o)) - [SOC_i + w(s_i^d) - e(s_i^d, s_j^o)] \tag{29}$$

The implicit expressions of $f(t)$ and $f^{-1}(SOC)$ in $FunSOC$ make it cumbersome to find the optimal solution to [ND-CS $_{ij}$] by standard approaches. Luckily, by making use of the concavity of the nonlinear charging profile, we can readily obtain the non-dominated charging strategy detailed in the following proposition.

Proposition 1: *A charging strategy for the link* ij *is non-dominated if*

Case 1: $SOC_i \geq e(s_i^d, s_j^o) + SOC_{min}$

An EV is relocated directly to the pick-up station of rental j *without charging at the drop-off station of rental* i *, i.e.,* $\tau^*(s_i^d) = 0$*, and then is charged at the pick-up station of rental* j *from the initial SOC at* $SOC_i - e(s_i^d, s_j^o)$ *for* $\tau^*(s_j^o) = \min\{FunTime(SOC_i - e(s_i^d, s_j^o), SOC_{max}), (t_j^o - t_i^d) - \tau(s_i^d, s_j^o)\}$ *. The SOC at the departure time clock of rental* j *is calculated by*

$$SOC_j^o(SOC_i, m_{ij}^*) = FunSOC(SOC_i - e(s_i^d, s_j^o), \tau^*(s_j^o)) \quad (30)$$

Case 2: $SOC_i < e(s_i^d, s_j^o) + SOC_{min}$

An EV is first charged at the drop-off station of rental i *until the SOC reaches* $e(s_i^d, s_j^o) + SOC_{min}$*, i.e.,* $\tau^*(s_i^d) = FunTime(SOC_i, e(s_i^d, s_j^o) + SOC_{min})$*, and then is relocated to the pick-up station of rental* j *for further charging from* SOC_{min} *for* $\tau^*(s_j^o) = \min\{FunTime(SOC_{min}, SOC_{max}), (t_j^o - t_i^d) - \tau(s_i^d, s_j^o) - \tau^*(s_i^d)\}$ *. The SOC at the departure time clock of rental* j *is calculated by*

$$SOC_j^o(SOC_i, m_{ij}^*) = FunSOC(SOC_{min}, \tau^*(s_j^o)) \quad (31)$$

Proof. We will demonstrate in the aforementioned two cases that for any feasible link ij, it holds that

$$SOC_j^o(SOC_i, m_{ij}^*) \geq SOC_j^o(SOC_i, m_{ij}), \forall m_{ij} \in M_{ij} \quad (32)$$

Case 1: $SOC_i \geq e(s_i^d, s_j^o) + SOC_{min}$

For any feasible charging strategy $m_{ij} \in M_{ij}$ with $\tau(s_i^d) \geq 0$ and $\tau(s_j^o) \geq 0$, we have

$$SOC_j^o(SOC_i, m_{ij}) = FunSOC(SOC_i + w(s_i^d) - e(s_i^d, s_j^o), \tau(s_j^o)) \quad (33)$$

where $w(s_i^d) = FunSOC(SOC_i, \tau(s_i^d)) - SOC_i$, $\tau(s_i^d) \le FunTime(SOC_i, SOC_{max})$, $\tau(s_j^o) \le FunTime(SOC_i + w(s_i^d) - e(s_i^d, s_j^o), SOC_{max})$ and

$$\tau(s_j^o) \le (t_j^o - t_i^d) - \tau(s_i^d, s_j^o) - \tau(s_i^d) \tag{34}$$

The expression of $SOC_j^o(m_{ij}^*)$ in Eq. (30) for the charging strategy m_{ij}^* is copied as follows,

$$SOC_j^o(SOC_i, m_{ij}^*) = FunSOC(SOC_i - e(s_i^d, s_j^o), \tau^*(s_j^o)) \tag{35}$$

It can been seen that the initial SOC before charging at the pick-up station of rental j in Eq. (33) is no less than that of Eq. (35), i.e., $SOC_i + w(s_i^d) - e(s_i^d, s_j^o) \ge SOC_i - e(s_i^d, s_j^o)$. Let τ denote the time required to charge from $SOC_i - e(s_i^d, s_j^o)$ to $SOC_i + w(s_i^d) - e(s_i^d, s_j^o)$, it follows that

$$\tau = FunTime(SOC_i - e(s_i^d, s_j^o), SOC_i + w(s_i^d) - e(s_i^d, s_j^o)) \ge 0 \tag{36}$$

and

$$SOC_j^o(SOC_i, m_{ij}^*) = FunSOC(SOC_i + w(s_i^d) - e(s_i^d, s_j^o), \tau^*(s_j^o) - \tau) \tag{37}$$

Since $\tau(s_i^d) = FunTime(SOC_i, SOC_i + w(s_i^d))$, according to decreasing charging efficiency during the CV phase, we have

$$\tau(s_i^d) \ge \tau \tag{38}$$

If $(t_j^o - t_i^d) - \tau(s_i^d, s_j^o) \le FunTime(SOC_i - e(s_i^d, s_j^o), SOC_{max})$, it follows from the description of charging strategy in Case 1 that $\tau^*(s_j^o) = (t_j^o - t_i^d) - \tau(s_i^d, s_j^o)$. Together with Eq. (34) and (38), we have

$$\tau(s_j^o) \le (t_j^o - t_i^d) - \tau(s_i^d, s_j^o) - \tau(s_i^d) \le \tau^*(s_j^o) - \tau \tag{39}$$

Hence, $SOC_j^o(SOC_i, m_{ij}) \le SOC_j^o(SOC_i, m_{ij}^*)$ according to Eq. (33) and Eq. (37).

If $(t_j^o - t_i^d) - \tau(s_i^d, s_j^o) > FunTime(SOC_i - e(s_i^d, s_j^o), SOC_{max})$, it follows that

$$SOC_j^o(SOC_i, m_{ij}^*) = SOC_{max} \ge SOC_j^o(SOC_i, m_{ij}) \tag{40}$$

Therefore we can conclude that Eq. (32) holds in Case 1.

Case 2: $SOC_i < e(s_i^d, s_j^o) + SOC_{min}$

It can be seen that an EV should be charged at the drop-off station of rental i for at least $\tau^*(s_i^d) = FunTime(SOC_i, e(s_i^d, s_j^o) + SOC_{min})$, otherwise the electricity would not be sufficient to support traveling from the drop-off station of rental i to the pick-up station of rental j. Therefore for any feasible charging strategy $m_{ij} \in M_{ij}$, we have $(t_j^o - t_i^d)$. Without considering the common charging duration of $\tau^*(s_i^d)$ at the pick-up station of rental i, we can find that seeking a feasible charging strategy under Case 2 is equivalent to finding a charging strategy under Case 1 with SOC_i and $(t_j^o - t_i^d)$ in Case 1 replaced by $e(s_i^d, s_j^o) + SOC_{min}$ and $(t_j^o - t_i^d) - \tau^*(s_i^d)$ in Case 2. Hence based on the demonstration for Case 1, the conclusion that $SOC_j^o(m_{ij}^*) \geq SOC_j^o(m_{ij}), \forall m_{ij} \in M_{ij}$ also holds in Case 2. □

Proposition 1 suggests that the realization of the non-dominated charging strategy depends on SOC_i. In other words, the non-dominated charging strategy is actually a vector function of SOC_i. It is also worth noting that the proposed non-dominated charging strategy is only viable for concave charging profiles. This, however, does not affect the applicability of the proposed approach because the realistic charging profiles generated by both the dominating charging schemes, i.e., the CC-CV and CP-CV scheme, are concave. As a special case, under a linear charging profile assumed by most previous studies, all the charging strategies would be non-dominated, and the feasibility of a trip chain will not be affected by the charging strategy applied to it. Analogous to the non-dominated charging strategy defined for a link, we have the following definition for the non-dominated charging strategy of a path.

Definition 4: For a path with the covered trips known a prior, we define that a charging strategy is non-dominated if the SOC at the departure time of its last rental is no less than that by any other feasible charging strategies for that path.

The following proposition reveals that a charging strategy for a path is non-dominated if the charging strategies of all the links along that path are non-dominated. This proposition helps to eliminate the exponential growth of labels resulted from the infinite number of feasible charging strategies, and thus plays an important role in solving the pricing problem. In particular, let Q_r be the set of feasible charging strategy for path r traversing node $i_1, i_2, ..., i_{n_r}$

in order, $SOC^o_{i_k}(SOC_{init}, q_r)$ be the SOC at the departure time clock of rental i_k after setting off from the pick-up station of the first rental i_1 at SOC_{init} and being charged by any charging strategy $q_r = \left\{m_{i_k i_{k+1}}\right\}_{k=1,2,...,n_r-1} \in Q_r$, and $q_r^* = \left\{m^*_{i_k i_{k+1}}\right\}_{k=1,2,...,n_r-1}$ be the non-dominated charging strategy defined in Definition 4; then we have the following proposition:

Proposition 2: *Given the initial SOC at SOC_{init}, for any feasible path with the covered trips $i_1, i_2, ..., i_{n_r}$, we have*

$$SOC^o_{i_{n_r}}(SOC_{init}, q_r^*) \geq SOC^o_{i_{n_r}}(SOC_{init}, q_r), \forall q_r \in Q_r \qquad (41)$$

Proof. We use mathematical induction to prove this proposition. In particular, we will demonstrate that if $SOC^o_{i_k}(SOC_{init}, q_r^*) \geq SOC^o_{i_k}(SOC_{init}, q_r)$ for rental i_k holds, then $SOC^o_{i_{k+1}}(SOC_{init}, q_r^*) \geq SOC^o_{i_{k+1}}(SOC_{init}, q_r)$ for the subsequent rental i_{k+1} would definitely hold.

Specifically, for $k = 1$, we have

$$SOC^o_{i_1}(SOC_{init}, q_r^*) = SOC^o_{i_1}(SOC_{init}, q_r) = SOC_{init} \qquad (42)$$

Let's assume that for any $k = 1, 2, ..., n_r - 1$, we have

$$SOC^o_{i_k}(SOC_{init}, q_r^*) \geq SOC^o_{i_k}(SOC_{init}, q_r) \qquad (43)$$

It follows from the definitions of the link and path charging strategy that

$$SOC^o_{i_{k+1}}(SOC_{init}, q_r^*) = SOC^o_{i_{k+1}}(SOC^o_{i_k}(SOC_{init}, q_r^*) - e_{i_k}, m^*_{i_k i_{k+1}}) \qquad (44)$$

$$SOC^o_{i_{k+1}}(SOC_{init}, q_r) = SOC^o_{i_{k+1}}(SOC^o_{i_k}(SOC_{init}, q_r) - e_{i_k}, m_{i_k i_{k+1}}) \qquad (45)$$

Since $SOC^o_j(SOC_i, m^*_{ij})$ is an non-decreasing function with respect to SOC_i, it holds based on Eq. (43) that

$$SOC^o_{i_{k+1}}(SOC^o_{i_k}(SOC_{init}, q_r^*) - e_{i_k}, m^*_{i_k i_{k+1}}) \geq SOC^o_{i_{k+1}}(SOC^o_{i_k}(SOC_{init}, q_r) - e_{i_k}, m^*_{i_k i_{k+1}}) \qquad (46)$$

Proposition 1 has demonstrated that

$$SOC^o_{i_{k+1}}(SOC^o_{i_k}(SOC_{init}, q_r) - e_{i_k}, m^*_{i_k i_{k+1}}) \geq SOC^o_{i_{k+1}}(SOC^o_{i_k}(SOC_{init}, q_r) - e_{i_k}, m_{i_k i_{k+1}}) \qquad (47)$$

By combining the Eq. (46) and (47), we have

$$SOC^o_{i_{k+1}}(SOC^o_{i_k}(SOC_{init}, q^*_r) - e_{i_k}, m^*_{i_k i_{k+1}}) \geq SOC^o_{i_{k+1}}(SOC^o_{i_k}(SOC_{init}, q_r) - e_{i_k}, m_{i_k i_{k+1}}) \quad (48)$$

which suggests that $SOC^o_{i_{k+1}}(SOC_{init}, q^*_r) \geq SOC^o_{i_{k+1}}(SOC_{init}, q_r)$ according to Eqs. (44) and (45). Therefore we can conclude that $SOC^o_{i_k}(SOC_{init}, q^*_r) \geq SOC^o_{i_k}(SOC_{init}, q_r)$ for any $k = 1, 2, ..., n_r$.

□

Proposition 2 verifies our conjecture that an optimal solution to the EVSPP-N&PR can be found by only generating labels by non-dominated charging strategy for each link, because it is consistent with the dominance test and the rationale for only retaining non-dominated labels within the multi-label method. There is no need to generate the labels/partial paths by all the other charging strategies because they would never dominate a label/partial path traversing the same sequence of nodes generated by non-dominated charging strategy. In addition, if there exist no feasible non-dominated charging strategies for a link, e.g., $(t^o_j - t^d_i) - \tau(s^d_i, s^o_j) - \tau^*(s^d_i) < 0$ in Case 2, the relocation operation from the drop-off station of rental i to the pick-up station of rental j can never become feasible by implementing any other charging strategies. The findings justify a tangible approach for pre-processing and feasibility check of labels within the multi-label method. The reinforced pre-processing procedure in Subsection 4.1.1 can be realized by first checking the existence of non-dominated charging strategy m^*_{ij} of link ij when departing from the pick-up station of rental i at SOC_{max}, and then examining whether $SOC^o_j(SOC_{max}, m^*_{ij}) - e_j \geq SOC_{min}$ holds if the non-dominated charging strategy does exist. Similarly, the feasibility of a (partial) path generated by the multi-label method can be checked by examining the existence of non-dominated charging strategy and the value of SOC_{i_j}.

4.1.3. Multi-label correcting method for solving the EVSPP-N&PR

Although the existing multi-label method for solving the MCPPR can work either in a label-setting or label-correcting way, only label correcting method is suitable for the EVSPP-N&PR. This is because (i) the possible existence of negative node cost makes the label setting method infeasible, and (ii) the rental sorting performed in the pre-processing procedure gives a clear ordering for label updating in a label correcting way.

To implement the multi-label method, each node $i \in \mathcal{I}$ is assumed to be associated with multiple labels representing partial paths ending at the drop-off station of rental i. We code any label k at the node i as $l_k(i) := [\hat{c}_k, \hat{w}_k, \gamma_k, \kappa_k]$, where $\hat{c}_k$ and $\hat{w}_k$ are the cost and SOC of the corresponding path respectively; γ_k and κ_k are the node and label index that precede label k and would be used to identify the traversed nodes of that path by backtrace. All these labels at node i are grouped into a set denoted by $\mathcal{L}(i)$.

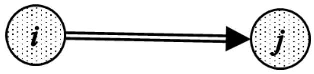

Figure 4. Two rentals with a link

The example in Figure 4 is used to illustrate the label updating process. Suppose we have label k at node i represented by $l_k(i) = [\hat{c}_k, \hat{w}_k, \gamma_k, \kappa_k]$; then a label denoted by $l_u(j) = [\hat{c}_k + c_j + c_{ij}, SOC_j^o(\hat{w}_k, m_{ij}^*) - e_j, i, k]$ at node j will be generated if there exists a non-dominated charging strategy for link ij. Once a new label is generated, the feasibility check and dominance test are performed successively. For the feasibility check, if $SOC_j^o(\hat{w}_k, m_{ij}^*) - e_j \geq SOC_{min}$ holds, the label will be retained, and discarded otherwise. The dominance test is to discard the labels at node j that are dominated by any other labels at that node in terms of the profit and SOC. The procedure of label correcting method for EVSPP-N&PR in the network $\mathcal{G} = (\mathcal{I}, \mathcal{A})$ with the initial SOC at SOC_{init} is summarized in Algorithm 1.

Algorithm 1: Pseudocode of label correcting method for EVSPP-N&PR

Initialize $\mathcal{L}(i) \leftarrow \varnothing$ for all $i \in \mathcal{I}$;
For each $i \in \mathcal{I}$ Do
    $\mathcal{L}(i) \leftarrow [c_i, SOC_{init} - e_i, 0, 0]$;
EndFor
For each $i \in \mathcal{I}$ Do
    $\mathcal{L}(i) \leftarrow$ *DominanceTest*($\mathcal{L}(i)$);
    For each $j \in \mathcal{I}$ and $ij \in \mathcal{A}$ Do
        For $k = 1$ to card($\mathcal{L}(i)$) Do
            $SOC_j^o \leftarrow$ *NondominatedChargeStrategy*($\hat{w}_k, e(s_i^d, s_j^o), \tau(s_i^d, s_j^o), t_i^d, t_j^o$);
            If $SOC_j^o - e_j \geq SOC_{min}$ Then

$\mathcal{L}(j) \leftarrow [\hat{c}_k + c_j + c_{ij}, SOC_j^o - e_j, i, k]$;

EndIf

EndFor

EndFor

EndFor

$(i^*, k^*) \leftarrow \arg \min_{i \in \mathcal{I}, l_k \in \mathcal{L}(i)} \{\hat{c}_k\}$ //node & label index of most profitable trip chain

---

Note that the *DominanceTest* and *NondominatedChargeStrategy* in Algorithm 1 are two subfunctions to perform the dominance test and to find the non-dominated charging strategy of a link, respectively. According to Proposition 1, SOC_j^o by the non-dominated charging strategy can be readily found given the values of $\hat{w}_k, e(s_i^d, s_j^o), \tau(s_i^d, s_j^o), t_i^d, t_j^o$, otherwise *NondominatedChargeStrategy* would return zero as the value of SOC_j^o. It should be noted that although the multi-label method for solving the EVSPP-N&PR works in a label correcting way, the ascending ordering of rentals guarantees that the generated labels are permanent even in a network with negative node cost. This feature greatly reduces the unnecessary label updating, and accordingly the feasibility check and dominance test within the multi-label method, and thus significantly improve the computational efficiency of the proposed label correcting method.

4.2. Tailing-off Effect

The optimal solution to the MP found by the column generation method provides an upper bound for the model [EVFS]. However, the column generation method often suffers from poor convergence, and only little progress per iteration is made when approaching the optimum. This phenomenon is referred to as the tailing-off effect in the literature (Ben Amor et al. 2006). Therefore, in practice the column generation process can be terminated once the gap between the current objective value and its optimal value is within a pre-specified tolerance ε_1. It is not difficult to demonstrate the following proposition by considering the dual problem of the MP.

Proposition 3: *Suppose that in an iteration of the column generation process, the optimal objective value of the RMP is* $LpObj$*, and the corresponding largest reduced cost satisfies* $P^* \le \frac{LpObj \times \varepsilon_1}{M}$ *where* $M \ge |\mathcal{I}|$*. Then* $LpObj \times (1 + \varepsilon_1)$ *is an upper bound on the MP.*

Proof. Let $\{\pi_i^*\}_{i\in\mathcal{I}}$ be the optimal dual value of constraint (14) in the current iteration of RMP, and $(\lambda,\pi_i)_{i\in\mathcal{I}}$ be the dual variables for the MP at the root node reformulated by imposing an additional constraint $\sum_{r\in\mathcal{R}} x_r \le M$ as follows:

[EVFS-MP-R]

$$\max_{x_r} \quad PROFIT_{new} = \sum_{r\in\mathcal{R}} (R_r - E_r - EC + \sum_{i\in\mathcal{I}} \delta_r^i P_i) x_r \tag{49}$$

subject to

$$\sum_{r\in\mathcal{R}} x_r \le M \tag{50}$$

$$\sum_{r\in\mathcal{R}} \delta_r^i x_r \le 1, \quad \forall i\in\mathcal{I} \tag{51}$$

$$x_r \ge 0, \quad \forall r\in\mathcal{R} \tag{52}$$

Since $M \ge |\mathcal{I}|$, the additional constraint will not affect the optimality of a solution because Eq. (50) would never be active at an optimal solution. In other words, the reformulated MP is equivalent to the original MP at optimality.

Since P^* is the largest reduced cost of the RMP, i.e., the optimal solution of problem [EVFS-PP] formulated by Eq. (17), we have $P^* \ge R_r - E_r - EC + \sum_{i\in\mathcal{I}} \delta_r^i P_i - \sum_{i\in\mathcal{I}} \delta_r^i \pi_i^*$, $\forall r\in\mathcal{R}\setminus\bar{\mathcal{R}}$. Besides, it follows from the duality theory that $P^* \ge R_r - E_r - EC + \sum_{i\in\mathcal{I}} \delta_r^i P_i - \sum_{i\in\mathcal{I}} \delta_r^i \pi_i^*, \forall r\in\bar{\mathcal{R}}$. Therefore, $(P^*,\pi_i^*)_{i\in\mathcal{I}}$ is a feasible solution to the dual problem of the model [EVFS-MP-R] formulated by

[EVFS-MP-R ^{dual}]

$$\min_{(\lambda,\pi_i)_{i\in\mathcal{I}}} \quad PROFIT_{new}^{dual} = \sum_{i\in\mathcal{I}} \pi_i + M\lambda \tag{53}$$

subject to

$$\lambda + \sum_{i\in\mathcal{I}} \delta_r^i \pi_i \ge R_r - E_r - EC + \sum_{i\in\mathcal{I}} P_i \delta_r^i, \forall r\in\mathcal{R} \tag{54}$$

$$\lambda \ge 0, \pi_i \ge 0, \forall i\in\mathcal{I} \tag{55}$$

Hence, the objective value of the model [EVFS-MP-R ^{dual}] at the feasible solution $(P^*, \pi_i^*)_{i\in\mathcal{I}}$ which equals $LpObj + M \times P^*$, is an upper bound for the optimal value of the model [EVFS-MP-R ^{dual}] since it is a minimization problem. Due to the strong duality theorem, the optimal values of the model [EVFS-MP-R ^{dual}] and [EVFS-MP-R] are equal. Hence, $LpObj \times (1+\varepsilon_1)$, which is not less than $LpObj + M \times P^*$, is an upper bound for [EVFS-MP-R] and thereby the upper bound for [EVFS-MP]. As a consequence of Proposition 3, the column generation process can be terminated faster without violating the relative optimality tolerance level ε_1.

□

It is worthwhile to note that a smaller M means a less number of iterations before terminating the column generation process, and Proposition 3 holds even with a M less than $|\mathcal{I}|$ as long as Eq. (50) would not be active at an optimal solution to [EVFS-MP]. In real applications, without knowing the real upper bound of the fleet size, we can choose a safe value $M := |\mathcal{I}|$ at the root node of B&P search tree, while an adaptive value of M detailed in the next subsection is employed at the non-root nodes in order to achieve the overall computational efficiency.

4.3. Tailored Branching Strategy

Since the solution to the MP may not be integer, branching operations are necessary to obtain an optimal integer solution to the model [EVFS]. The standard branching on the decision variable x_r results in an imbalanced search tree. Therefore we develop a tailored branching strategy based on the following proposition:

Proposition 4: *If an optimal solution to the MP is not integer, then there must exist either a rental* $i \in \mathcal{I}$ *such that* $0 < \sum_{r\in\mathcal{R}} \delta_r^i x_r < 1$ *or a pair of rental* $i, j \in \mathcal{I}$ *such that* $0 < \sum_{r\in\mathcal{R}(i,j)} x_r < 1$, *where* $\mathcal{R}(i, j)$ *denotes the set of trip chains covering both the rental* i *and rental* j.

Proof. The proposition can be proved by contradiction. Suppose that there exist no rentals $i \in \mathcal{I}$ such that $0 < \sum_{r\in\mathcal{R}} \delta_r^i x_r < 1$, and also no pairs of rentals $i, j \in \mathcal{I}$ such that $0 < \sum_{r\in\mathcal{R}(i,j)} x_r < 1$.

The former assumption suggests that

$$\sum_{r\in\mathcal{R}} \delta_r^i x_r^* = 1, \quad \forall i \in \mathcal{SI} \tag{56}$$

$$\sum_{r\in\mathcal{R}} \delta_r^i x_r^* = 0, \quad \forall i \in \mathcal{RI} \tag{57}$$

where x_r^* is the optimal solution to MP; $\mathcal{SI}$ and $\mathcal{RI}$ are the set of satisfied and rejected rentals respectively. Apparently, we have $\mathcal{SI} \cup \mathcal{RI} = \mathcal{I}$.

The latter assumption implies that we cannot identify a pair of rentals $i, j \in \mathcal{SI}$ such that $0 < \sum_{r\in\mathcal{R}(i,j)} x_r < 1$. Ryan and Foster (1981) formulated a set partitioning model for the bus crew scheduling problem, and they have rigorously demonstrated that in the aforementioned case, the solution to the MP must be integer. Therefore the conclusion of this proposition holds. □

Proposition 4 suggests the following branching strategy for the MP:

Case 1:

If there exists a rental $i \in \mathcal{I}$ such that $0 < \sum_{r\in\mathcal{R}} \delta_r^i x_r < 1$, we branch on this rental in a way that on the left branch, we require that rental i must be satisfied by the fleet of EVs, i.e., $\sum_{r\in\mathcal{R}} \delta_r^i x_r = 1$, and on the right branch, we reject to satisfy rental i, i.e., $\sum_{r\in\mathcal{R}} \delta_r^i x_r = 0$.

Case 2:

If there exist no rentals such that $0 < \sum_{r\in\mathcal{R}} \delta_r^i x_r < 1$, we can identify and branch on a pair of rentals i, j such that $0 < \sum_{r\in\mathcal{R}(i,j)} x_r < 1$. On the left branch, we require that rental i and rental j must be covered by a same trip chain, i.e., $\sum_{r\in\mathcal{R}(i,j)} x_r = 1$, and on the right branch, rental i and rental j are not allowed to be covered by a same trip chain, i.e., $\sum_{r\in\mathcal{R}(i,j)} x_r = 0$.

Desrochers and Soumis (1998) proposed an alternative branching strategy for Case 2, in which $\mathcal{R}(i, j)$ is replaced by $\mathcal{Q}(i, j)$ denoting the set of trip chains covering the rental i and rental j successively. In light of its easy implementation in our pricing problem, we will employ the alternative branch strategy in Case 2.

With the tailored branching strategy, the B&P approach will terminate with an optimal integer solution after a finite number of branches. Let $\mathcal{IP}$ and $\mathcal{EP}$ denote the sets of included and excluded pairs of rentals respectively. As the algorithm proceeds, the MP at a node would be associated with a long list of rentals in $\mathcal{SI}$ and $\mathcal{RI}$ as well as a long list of rental pairs in

$\mathcal{IP}$ and $\mathcal{EP}$. The sets $\mathcal{SI}$ and $\mathcal{RI}$ would change the constraint (14) of MP to be

$$\sum_{r\in\mathcal{R}} \delta_r^i x_r = 1, \quad \forall i \in \mathcal{SI} \tag{58}$$

$$\sum_{r\in\mathcal{R}} \delta_r^i x_r = 0, \quad \forall i \in \mathcal{RI} \tag{59}$$

$$\sum_{r\in\mathcal{R}} \delta_r^i x_r \le 1, \quad \forall i \in \mathcal{I} \setminus (\mathcal{SI} \cup \mathcal{RI}) \tag{60}$$

It can be seen that Constraint (59) can be eliminated without affecting the solution of MP if we exclude all the rentals in $\mathcal{RI}$ from the pricing problem. The list of pairs of rentals that should be excluded or included can also be incorporated in the pricing problem by network reconstruction. To be specific, for each pair of rentals that should be excluded, we will delete the corresponding link in the network, while for each pair of rentals that should be included, we will retain the corresponding link and delete all the other links originating from the tail of corresponding link. As for the long tail effect, Proposition 3 holds for a MP with constraints (58)-(60). However, the value of M can be reduced to $|\mathcal{I}| - |\mathcal{RI}| - |\mathcal{IP}|$ at a node associated with sets $\mathcal{SI}$, $\mathcal{RI}$, $\mathcal{IP}$ and $\mathcal{EP}$.

4.4. Tailored Branch-and-Price Method

The step-by-step procedure of the tailored B&P method is summarized as follows:

Step 0: (Initialization) Define the relative optimality tolerances associated with column generation and branching denoted by ε_1 and ε_2 respectively. Initialize the lower bound $LB := 0$. The binary tree $\mathcal{T}$ consists of only a root node n_0. The corresponding MP, denoted by MP(n_0) is associated with a set of initial columns defined by $\bar{\mathcal{R}}(n_0) := \{r_i, \forall i \mid \delta_{r_i}^i = 1 \wedge \delta_{r_i}^{i'} = 0, \forall i' \in \mathcal{I} \setminus i\}$, a set of satisfied rentals initilized by $\mathcal{SI}(n_0) := \varnothing$, a set of rejected rentals denoted by $\mathcal{RI}(n_0) := \varnothing$, a set of included pairs of rentals denoted by $\mathcal{IP}(n_0) := \varnothing$, and a set of excluded pairs of rentals denoted by $\mathcal{EP}(n_0) := \varnothing$. The upper bound for the root node is defined by $UB(n_0) := +\infty$. The upper bound for the fleet size at the root node is defined by $M(n_0) := |\mathcal{I}|$. Node n_0 is marked as an active node. Initialize the incumbent feasible solution $x_r^{incu} := NULL, \forall r$.

Step 1: (Node exploration) An incumbent node denoted by n is first selected from all the active nodes in the binary tree by the depth-first and back-tracking search rule.

Step 2: (Solve MP by column generation)

- ***Step 2.0:*** Set the iteration number $k := 1$ and denote the subset of trip chains at iteration k by $\bar{\mathcal{R}}(n,k)$. Initialize $\bar{\mathcal{R}}(n,1) := \bar{\mathcal{R}}(n)$.
- ***Step 2.1:*** Solve the RMP of node n at k^{th} iteration formulated by

[RMP(n,k)]:

$$\max_{\{x_r, r\in\bar{\mathcal{R}}(n,k)\}} \sum_{r\in\bar{\mathcal{R}}(n,k)} (R_r - E_r - EC + \sum_{i\in\mathcal{I}} \delta_r^i P_i) x_r \tag{61}$$

subject to

$$\sum_{r\in\bar{\mathcal{R}}(n,k)} \delta_r^i x_r = 1, \quad \forall i \in \mathcal{SI}(n) \tag{62}$$

$$\sum_{r\in\bar{\mathcal{R}}(n,k)} \delta_r^i x_r = 0, \quad \forall i \in \mathcal{RI}(n) \tag{63}$$

$$\sum_{r\in\bar{\mathcal{R}}(n,k)} \delta_r^i x_r \le 1, \quad \forall i \in \mathcal{I} \setminus (\mathcal{SI}(n) \bigcup \mathcal{RI}(n)) \tag{64}$$

$$x_r \ge 0, \quad \forall r \in \bar{\mathcal{R}}(n,k) \tag{65}$$

Let $LpObj(n,k)$ be the optimal objective value at the current iteration. Obtain the dual variables. Construct the pseudo-network for the set of rentals $\mathcal{I} \setminus \mathcal{RI}(n)$. Invoke the multi-label method for EVSPP-N&PR considering the sets $\mathcal{SI}(n)$, $\mathcal{RI}(n)$, $\mathcal{IP}(n)$, $\mathcal{EP}(n)$, and obtain the optimal trip chain denoted by $r^*(n,k)$ and its corresponding profit denoted by $P(r^*)$. If $P(r^*) > \dfrac{LpObj(n,k)\times\varepsilon_1}{M(n)}$, then set $\bar{\mathcal{R}}(n,k+1) := \bar{\mathcal{R}}(n,k) \bigcup \{r^*(n,k)\}$, $k := k+1$ and repeat Step 2.1. Otherwise let $x_r^*(n), \forall r$ be the optimal solution to the model [RMP(n,k)] and $LpObj(n) := LpObj(n,k)$; let $\mathcal{R}(n) := \bar{\mathcal{R}}(n,k)$ denote the final set of columns at node n and go to Step 3.

Step 3: (check integrality and update lower bound) If $x_r^*(n), \forall r$ are all integer and $LpObj(n) \le LB$, mark node n as inactive node and go to Step 6; If $x_r^*(n), \forall r$ are all integer and $LpObj(n) > LB$, update the incumbent feasible solution $x_r^{incu} := x_r^*(n), \forall r$, set $LB = LpObj(n)$, search the whole tree and mark all active nodes n' satisfying

$UB(n') \le (1+\varepsilon_2) \times LB$ as inactive (node n is also marked as inactive node) and go to Step 6. Otherwise, go to Step 4.

Step 4: (Node fathoming) If $LpObj(n) \le (1+\varepsilon_2) \times LB$, node n is marked as inactive node and go to Step 6, otherwise go to Step 5.

Step 5: (Node branching)

If there exists a rental i^* such that

$$i^* := \arg \max_{i \in \mathcal{I} \setminus [\mathcal{SI}(n) \cup \mathcal{RI}(n)]} \left\{ \sum_{r \in \mathcal{R}(n)} \delta_r^i x_r^*(n) \,|\, \sum_{r \in \mathcal{R}(n)} \delta_r^i x_r^*(n) < 1 \right\} \tag{66}$$

then the node is branched into two child nodes, denoted by n_1 and n_2. Nodes n_1 and n_2 copy all the information from node n except that for node n_1 we have $\mathcal{SI}(n_1) := \mathcal{SI}(n) \cup \left\{ i^* \right\}$ and $UB(n_1) := LpObj(n)$; for node n_2 , we have $\bar{\mathcal{R}}(n_2) := \left\{ r \in \mathcal{R}(n) \,|\, \delta_r^{i^*} = 0 \right\}$, $\mathcal{RI}(n_2) := \mathcal{RI}(n) \cup \left\{ i^* \right\}$, $UB(n_2) := LpObj(n)$ and $M(n_2) := M(n) - 1$. Both nodes are marked as active nodes.

Otherwise we can identify a pair of rentals (i_a^*, i_b^*) such that

$$(i_a^*, i_b^*) \in \arg \max_{i_a, i_b \in \mathcal{SI}(n)} \left\{ \sum_{r \in \mathcal{Q}(i_a, i_b) \subseteq \mathcal{R}(n)} \delta_r^i x_r^*(n) \,|\, \sum_{r \in \mathcal{Q}(i_a, i_b) \subseteq \mathcal{R}(n)} \delta_r^i x_r^*(n) < 1 \right\} \tag{67}$$

The node is branched into two child nodes, denoted by n_1 and n_2. Nodes n_1 and n_2 copy all the information from node n except that for node n_1 we have $\mathcal{IP}(n_1) := \mathcal{IP}(n) \cup \left\{ (i_a^*, i_b^*) \right\}$, $UB(n_1) := LpObj(n)$ and $M(n_1) := M(n) - 1$; for node n_2 , we have $\mathcal{EP}(n_2) := \mathcal{EP}(n) \cup \left\{ (i_a^*, i_b^*) \right\}$ and $UB(n_1) := LpObj(n)$. Both nodes are marked as active nodes.

Step 6: (Stop criterion) If all the nodes in the binary tree become inactive, stop and output the incumbent feasible solution $x_r^{incu}, \forall r$ and the corresponding lower bound LB. Otherwise, go to Step 1.

5. Two Heuristic Methods

The B&P method is computationally intractable for large-size problems due to the NP-hardness. Hence it is necessary to develop heuristics to find an approximate solution in a reasonable amount of time. In this section, two heuristic methods are proposed. One method is adapted from the concurrent scheduler algorithm pioneered by Bodin et al. (1978). The other heuristic method, referred to as the MILP-based heuristic method, is to directly solve the model [EVFS] with the columns generated at the root node of the B&B tree. The solutions obtained by the two heuristic methods may provide a set of promising initial columns and/or a tight lower bound for B&P approach.

The concurrent scheduler algorithm assigns trips to vehicles in a greedy way. In the context of carsharing, for example, the algorithm assigns the first rental to a vehicle, then iteratively treat the rentals in order. The feasibility check and/or incremental cost calculation are performed when assigning a particular rental to an existing vehicle or a new vehicle. The trip would be assigned to a feasible vehicle with the highest incremental profit to fleet operators. When applying the heuristics, special consideration should be given to EVFS problem due to the negative cost and the flexibility to reject a rental. In particular, for an existing vehicle with already assigned rental(s), if its incumbent profit denoted by $PROFIT^{incumbent}$ is non-negative, the incremental profit for assigning an additional rental j after the last rental i of the trip chain should be calculated by $PROFIT^{incremental} = G_j - OC_j + P_j - UC \times e(s_i^d, s_j^o)$, otherwise the incremental profit should be $PROFIT^{incumbent} + PROFIT^{incremental}$. The reason for calculating the total profit of a partial trip chain as the incremental profit of a rental in latter case is attributed to the consideration that the profit of a trip chain may make no contribution to the total profit of carsharing operators if its final profit is negative. Therefore among all the feasible partial trip chains with negative incumbent profit, the one with the greatest potential to become a final profitable trip chain by connecting its last rental with the additional rental is the most preferred alternative. The empirical studies have justified the effectiveness of calculating the incremental profit differently according to the sign of incumbent profit of a partial trip chain. In addition, after all the rentals have been assigned to EVs, only the trip chains with positive profit would be chosen as the final solution to EVFS. Apart from above considerations, the non-dominated charging strategy should also be adopted when connecting two rentals.

For ease of illustration, let $\mathcal{V}$ denote the set of existing EVs/partial trip chains and v_{new} represent a new EV. Any EV $v \in \mathcal{V}$ is associated with three values, i.e., the index of the last rental of the partial trip chain denoted by i_v, the value of SOC after arriving at the drop-off station of rental i_v denoted by SOC_v, the incumbent profit of the partial trip chain denoted by $PROFIT_v^{incumbent}$. Let $PROFIT_v^{incremental}$ denote the incremental profit for assigning an additional rental after the last rental of the trip chain. With the above notations, Algorithm 2 outlines the procedure of concurrent scheduler based heuristic for the EVFS problem with the initial SOC at SOC_{init}.

Algorithm 2: Pseudocode of concurrent scheduler based heuristic for the EVFS problem

---

Initialize $\mathcal{V} \leftarrow \varnothing$;
For each $j \in \mathcal{I}$ Do
  For each $v \in \mathcal{V}$ Do //iterate through existing trip chains
    If $\tau(s_{i_v}^d, s_j^o) \le t_j^o - t_{i_v}^d$ & $e(s_{i_v}^d, s_j^o) \le SOC_{max} - SOC_{min}$ Then //for time feasibility
      $SOC_{j(v)}^o \leftarrow NondominatedChargeStrategy(SOC_v, e(s_{i_v}^d, s_j^o), \tau(s_{i_v}^d, s_j^o), t_{i_v}^d, t_j^o)$;
      If $SOC_{j(v)}^o - e_j \ge SOC_{min}$ Then //for SOC feasibility
        If $PROFIT_v^{incumbent} \ge 0$ Then
          $PROFIT_v^{incremental} \leftarrow G_j - UC \times e_j + P_j - UC \times e(s_{i_v}^d, s_j^o)$;
        Else $PROFIT_v^{incremental} \leftarrow PROFIT_v^{incumbent} + G_j - UC \times e_j + P_j$
          $-UC \times e(s_{i_v}^d, s_j^o)$;
        EndIf
      Else $PROFIT_v^{incremental} \leftarrow -\infty$;
      EndIf
    Else $PROFIT_v^{incremental} \leftarrow -\infty$;
    EndIf
  EndFor
  $PROFIT_{v_{new}}^{incremental} \leftarrow G_j - UC \times e_j + P_j - EC$;
  $v^* = \arg\max_{v \in \mathcal{V} \cup \{v_{new}\}} PROFIT_v^{incremental}$;
  If $v^* \in \mathcal{V}$ Then //update an existing trip chain with an additional rental
    $i_{v^*} \leftarrow j$; $SOC_{v^*} = SOC_{j(v^*)}^o - e_j$;

If $PROFIT_{v^*}^{incumbent} \geq 0$ Then

$PROFIT_{v^*}^{incumbent} \leftarrow PROFIT_{v^*}^{incumbent} + PROFIT_{v^*}^{incremental}$;

Else $PROFIT_{v^*}^{incumbent} \leftarrow PROFIT_{v^*}^{incremental}$;

EndIf

Else $v_{new} \rightarrow \mathcal{V}$; $i_{v_{new}} \leftarrow j$; $SOC_{v_{new}} \leftarrow SOC_{init} - e_j$;

$PROFIT_{v_{new}}^{incumbent} \leftarrow PROFIT_{v_{new}}^{incremental}$; //generate a new trip chain

EndIf

EndFor

$\mathcal{V}^* \leftarrow \{v \in \mathcal{V} \mid PROFIT_v^{incumbent} > 0\}$ //set of near-optimal trip chains

---

The MILP-based heuristic method is particularly suitable to be implemented within the B&P approach as a reinforcement because it can generate a feasible solution and a tight bound within a fraction of a second. To this end, several modifications should be made in the B&P scheme. For example, in the Step 3 of the B&P scheme, if $x_r^*(n), \forall r$ are not all integer, before going to Step 4, we can invoke the MILP solver to solve [EVFS-MP] with $\mathcal{R}(n)$ and denote the optimal objective value by $MILPObj(n)$. If $MILPObj(n) > LB$, we can update the incumbent feasible solution $x_r^{incu} := x_r^*(n), \forall r$, set $LB = MILPObj(n)$, search the whole tree and mark all active nodes n' satisfying $UB(n') \leq (1+\varepsilon_2) \times LB$ as inactive. The proposed two methods for EVFS problem will be evaluated and compared with B&P approach in the numerical experiments.

6. Numerical Experiments

In this section, random instances are generated to evaluate the performance of the proposed B&P and heuristic methods. A case study created from SMOVE in Singapore is conducted to further assess the efficiency of the algorithms when implemented in a real case as well as to explore how the key parameters of electric carsharing services affect the system performance. The algorithms are coded in Matlab 2010b calling IBM ILOG CPLEX 12.6 on a personal computer with Intel (R) Core (TM) Duo 3.4 GHz CPU.

6.1. Randomly Generated Instances

We will generate a set of illustrative small-sized instances to assess the efficiency of the proposed solution methods as detailed in the following subsections.

6.1.1 Parameters Setup

In order to create the random instances, we first uniformly chose $|S|$ stations from a 50 km by 50 km grid. The pick-up and drop-off points of $|\mathcal{D}|$ rental requests, i.e., s_i^o and s_i^d, are randomly chosen from the generated stations. We further assume that the study period is from 7 am to 6 pm with more rentals required to depart in the first and last hours. Specifically, if 7 am is taken as the time benchmark and the time duration is measured in minutes, the departure time of each trip i, i.e., t_i^o, is an integer randomly chosen with a 15% probability of being from interval [0, 60), a 70% probability of being from interval [60, 600], and a 15% probability of being from interval (600, 660]. Let $dis(s_i^o, s_i^d)$ be the Euclidean distance between the pick-up station and the drop-off station of rental i. Given an average travel speed $v = 50$ km/hr, the minimum rental duration of trip i would be $dis(s_i^o, s_i^d)/v$ hrs. The arrival time of trip i, i.e., t_i^d, is thus chosen as a uniformly random integer from the set $\{dis(s_i^o, s_i^d)/v, dis(s_i^o, s_i^d)/v + 5\text{min}, ..., dis(s_i^o, s_i^d)/v + 30\text{min}\}$. The electricity consumption e_i, which is expressed in percentage to the maximum possible charge of battery installed in EVs, is randomly chosen from the interval $[dis(s_i^o, s_i^d)/v, t_i^d - t_i^o] \times dchar$, where $dchar$ is the discharge rate of battery and is assumed to be 30%/hr. This is roughly consistent with the reality that the traveled distance of Nissan Leaf 30 kWh (Nissan, 2018) in one hour is about 30% of its driving range (107 miles).

The meter fare of normal taxi in Singapore is about 0.46\$/min excluding the fare of flag down, waiting time and several surcharges (Taxi, 2018). We assume without loss of generality that the carsharing service is charged only by rental duration and the unit service charge is UR =0.30S\$/min, which remains more attractive than taxi service in the local context. Hence the revenue from rental i is calculated by $G_i = UR \times (t_i^d - t_i^o)$. The penalty of rejecting rental i, i.e., P_i, is assumed to be half of the revenue of that trip. The cost of trips only depend on the amount of electricity consumption. We assume the electricity cost for a fully charge of Nissan Leaf 30 kWh is 12S\$. The travel time and electricity consumption of relocation operation from the drop-off station of trip i to the pick-up station of trip j are calculated by $t(s_i^d, s_j^o) = dis(s_i^d, s_j^o)/v$ and $e(s_i^d, s_j^o) = t(s_i^d, s_j^o) \times dchar$, respectively. The relocation cost is assumed to be 0.3S\$/min. The fixed cost of EV is set to be $EC = 20S\$$ per vehicle-day. The

EVs are assumed to be fully charged at the very beginning of operation period, i.e., $SOC_{init} = SOC_{max}$. Both the SOC_{cutoff} and SOC_{comf} is set to be 1%. All the other parameters in the nonlinear charging profile are adopted from the numerical examples of Pelletier et al. (2017).

6.1.2. Assessment of Solution Methods

Various combinations of number of stations and rentals are used to test the performance of the B&P approach and two heuristic methods. The concurrent scheduler based heuristic is applied independently, whereas the MILP-based heuristic method is implemented within the B&P approach, referred to as MILP-reinforced B&P approach. For a particular combination of number of stations and rentals, ten instances are randomly generated and the average results are reported. The relative optimality gap is controlled by ε_1 and ε_2. By setting $\varepsilon_1 = \varepsilon_2 = 0.0005$, the overall relative optimality gap is about 0.1%.

Table 1 shows the results of the B&P approach, and each row corresponds to the average results obtained for the ten randomly generated instances for a particular problem size indicated by the number of rentals (#Rental) and stations (#Station) in the table. We report several parameters in the table, including the optimal EV fleet size (FS), the objective value of model [EVFS] (Obj), the CPU time to obtain the optimal solution (T_CPU Time), to generate columns (CG_CPU Time) and the ratio of CG_CPU Time to T_CPU Time (CG/T_CPU Time), the number of priced out columns/trip chains (#TC), the number of nodes traversed (#Node), the maximal depth level (#MaxLevel) and the maximal number of active nodes (#MaxNode) in the B&P search tree.

According to the total CPU time in the table for solving the EVFS problem, we can see that on average, the B&P approach can solve the small-size problems (less than 100 rentals) to optimality within one hour. However, the CPU time would increase rapidly as the number of rentals increases. Unlike the number of rentals that largely and negatively affects the computational efficiency of the B&P approach, the impact of station number appears smaller and somehow arbitrary. The ratio of CPU time by column generation to the total CPU time is no more than 30%. The average, however, hides much of the variability: the ratio reaches up to 80% in a few instances, suggesting that the efficiency of the B&P approach largely depends on the computational efficiency of column generation, i.e., the label correcting method for EVSPP-N&PR. The ratio of CPU time of column generation to the total number of column priced out reflects the average CPU time required for finding an additional column. It can be seen that both the number of columns priced out and the average CPU time per column increase apparently with the growing number of rentals, leading to a rapidly increased CPU time for column generation, and accordingly for the B&P approach. The number of nodes traversed and maximal depth level in the search tree generally measures the difficulty for solving a problem, while the maximal number of active nodes reflects the computer memory requirement for recording the information of a search tree. It can be seen from Table 1 that all these numbers are no more than a dozen, demonstrating the viability of the proposed method for solving EVFS.

Table 2 compares the performance of the B&P approach and the concurrent scheduler based heuristic in terms of the fleet size, the objective value of model [EVFS], and the total CPU time required to obtain the solution. For ease of comparison, we also report the difference of fleet size (Diff_FS) and the relative decrease of objective value (Diff_Obj) between the heuristic method and the B&P approach. It shows that the concurrent scheduler based heuristic obtains a solution with a fraction of a second, which may require thousands of seconds by B&P approach. The computational efficiency of the heuristic method appears non-sensitive to the number of rentals. These results suggest that the concurrent scheduler based heuristic significantly dominates the B&P approach both in terms of magnitude and variation of computation time. Regarding the quality of solution, the optimal fleet size achieved by the heuristic method is at most 2.5 more than that of B&P approach, and the difference of objective value is no more than 5.0%. The worst-case fleet size and objective value difference are 5 and 12.2% respectively. We also plot the histogram and empirical cumulative distribution curve in Figure 5. It shows that in most of instances the fleet size and objective value difference are no more than 2 and 6% respectively. Although the difference of objective value may not be neglected, it is not the major criterion for evaluating the algorithms because our main concern is the fleet size for the carsharing service. Therefore the results have demonstrated the efficiency and effectiveness of the proposed concurrent scheduler based heuristic in solving the EVFS problem.

Table 3 compares the performance of B&P approach and the MILP-reinforced B&P method in terms of total CPU time required to obtain the solution, the number of priced out columns/trip chains, the number of nodes traversed, the maximal depth level, and the maximal number of active node in the B&P search tree. The ratios of the total CPU time and the number of priced out columns by the MILP-reinforced B&P method over that by the B&P approach without reinforcement (minus 1) are also reported for ease of comparison. For the MILP-reinforced B&P approach, the additional CPU time in solving MILP at the root node

(MILP_CPU Time) is also tabulated. Note that the optimal fleet size and the objective value, and the results by MILP-based heuristic method are not reported in the table because they have no value of comparison or most values are mere repetitions of results already listed in Table 3. It can be observed that in most scenarios, only one node is traversed in the search tree of MILP-reinforced B&P method, indicating that the MILP-based heuristic method has already solved the EVFS problem to optimality at the root node and there is no need to branch. In fact, additional nodes in the B&P search tree are only generated in 6 out of 1500 test instances. Compared with the B&P approach, the MILP-reinforced B&P method obtains the optimal solution with less CPU time by pricing out a less number of columns, and reducing the number of nodes traversed and the maximal depth level in the B&P search tree, generally at the sacrifice of only a fraction of a second for solving an additional MILP, although there exists an exception in the scenario with 125 rentals and 40 stations where the MILP takes 191 seconds to solve. It can be seen that the reduction ratios of the total CPU time and the number of priced out columns reach as high as 46.3% and 50.2%, respectively.

The computational efficiency of the B&P approach is largely affected by the number of rentals, making it unsuitable for large-scale carsharing services in real applications. Although the MILP-reinforced B&P method averagely dominates the B&P approach without reinforcement by generating the same optimal solution with less CPU time, it may still not be applicable for large-scale problems as its CPU time can easily grow up to thousands of seconds. Therefore in real-world carsharing service such as SMOVE, we further investigate the performance of the proposed MILP-reinforced B&P method and the concurrent scheduler based heuristic in solving small-size problems, as well as the performance of concurrent scheduler based heuristic in solving large-scale problems.

Table 1. Results of EVFS problem by B&P approach on randomly generated instances

#Rental	#Station	FS	Obj (S$)	T_CPU Time (s)	CG_CPU Time (s)	CG/T_CPU Time	#TC	CG_CPU Time/#TC (s)	#Node	#MaxLevel	#MaxNode
25	20	5.7	309.3	204	3	1%	95	0.03	1.2	0.2	1.2
25	30	5.3	330.4	234	3	1%	113	0.03	1.4	0.4	1.4
25	40	5.8	336.0	192	2	1%	94	0.02	1	0	1
50	20	9.3	708.1	698	57	8%	387	0.15	2.8	1.8	2.8
50	30	8.2	688.6	979	65	7%	424	0.15	1.5	0.5	1.5
50	40	10.3	666.8	720	39	5%	322	0.12	1	0	1
75	20	12.3	1061.5	1782	269	15%	963	0.28	3.7	2.7	3.7
75	30	11.9	1126.3	2561	482	19%	1115	0.43	6.8	5	5.6
75	40	12.9	1071.3	1871	261	14%	716	0.36	1.6	0.6	1.6
100	20	15.8	1527.2	3345	729	22%	1255	0.58	8.7	7.3	8.3
100	30	15.9	1413.5	4404	814	18%	1206	0.67	4.8	3.8	4.8
100	40	15.4	1429.0	4262	742	17%	1317	0.56	3.8	2.8	3.8
125	20	19.7	1926.4	7327	2210	30%	2302	0.96	19.2	18.2	19.2
125	30	18.9	1803.0	7840	1892	24%	1695	1.12	4.1	3.1	4.1
125	40	19.9	1913.2	8820	1814	21%	1912	0.95	6.6	5.4	6.4

Table 2. Comparison of B&P and concurrent scheduler based heuristic on randomly generated instances

		B&P			Heuristic				
#Rental	#Station	FS	Obj (S$)	T_CPU Time (s)	FS	Diff_FS	Obj (S$)	Diff_Obj	T_CPU Time (s)
25	20	5.7	309.3	204	6.6	0.9	296.4	-4.2%	0.02
25	30	5.3	330.4	234	5.3	0	315.3	-4.6%	0.01

25	40	5.8	336.0	192	6.4	0.6	320.8	-4.5%	0.01
50	20	9.3	708.1	698	10.1	0.8	681.1	-3.8%	0.01
50	30	8.2	688.6	979	9.6	1.4	661.1	-4.0%	0.01
50	40	10.3	666.8	720	9.9	-0.4	656.1	-1.6%	0.02
75	20	12.3	1061.5	1782	13	0.7	1035.2	-2.5%	0.03
75	30	11.9	1126.3	2561	13.4	1.5	1093.5	-2.9%	0.02
75	40	12.9	1071.3	1871	13.3	0.4	1042.1	-2.7%	0.03
100	20	15.8	1527.2	3345	17.4	1.6	1485.4	-2.7%	0.04
100	30	15.9	1413.5	4404	18.4	2.5	1342.4	-5.0%	0.04
100	40	15.4	1429.0	4262	16.6	1.2	1391.5	-2.6%	0.04
125	20	19.7	1926.4	7327	21	1.3	1883.1	-2.2%	0.05
125	30	18.9	1803.0	7840	20.1	1.2	1754.6	-2.7%	0.05
125	40	19.9	1913.2	8820	21.3	1.4	1850.7	-3.3%	0.05

Figure 5. The histogram and histogram and empirical cumulative distribution curve of fleet size difference (Diff_FS) and objective value difference (Diff_Obj)

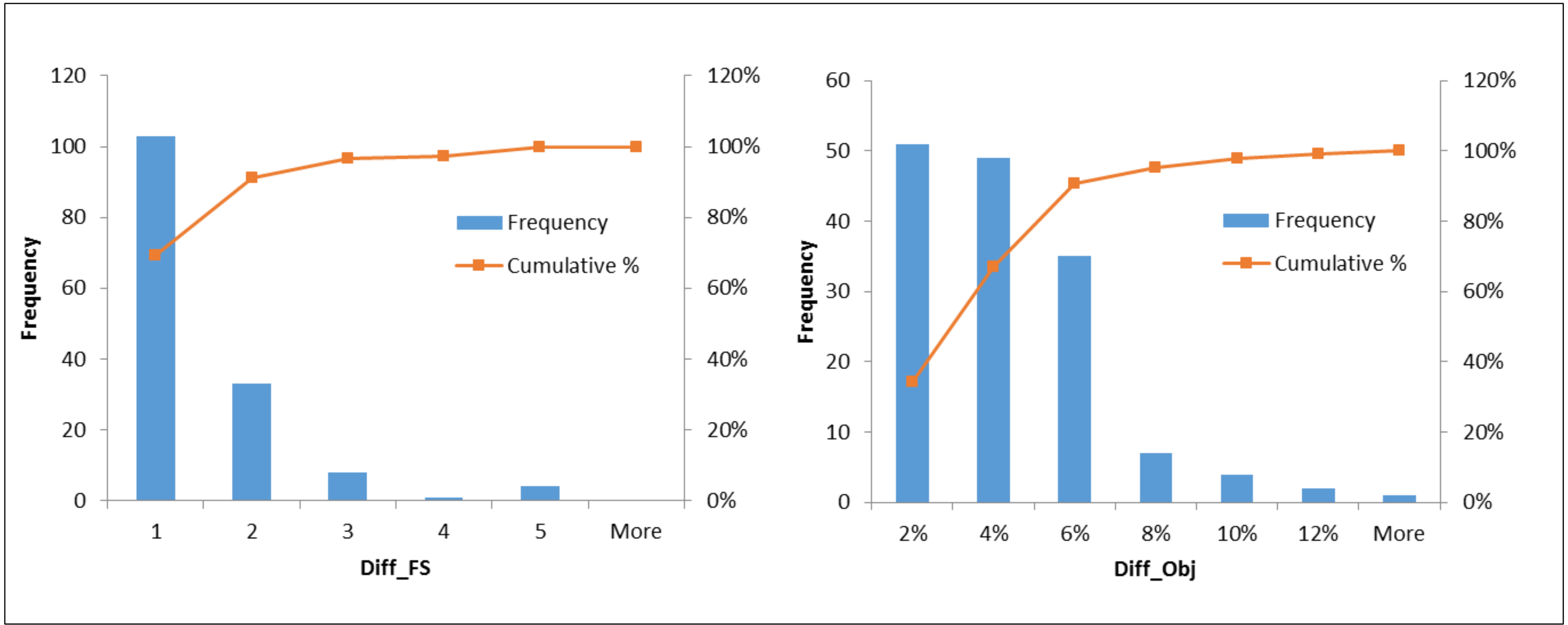

Table 3. Comparison of B&P and MILP-reinforced B&P on randomly generated instances

		B&P					MILP-reinforced B&P							
#Rental	#Station	T_CPU Time (s)	#TC	#Node	#MaxLevel	#MaxNode	T_CPU Time (s)	%T_CPU Time	#TC	%#TC	#Node	#MaxLevel	#MaxNode	MILP_CPU Time (s)
25	20	204	95	1.2	0.2	1.2	203	-0.52%	94	-0.32%	1.3	0.3	1.3	0.02
25	30	234	113	1.4	0.4	1.4	233	-0.32%	108	-4.26%	1	0	1	0.07
25	40	192	94	1	0	1	193	0.34%	94	0.00%	1	0	1	0.00
50	20	698	387	2.8	1.8	2.8	670	-4.03%	303	-21.75%	1	0	1	0.07
50	30	979	424	1.5	0.5	1.5	980	0.10%	414	-2.45%	1.2	0.2	1.2	0.16

50	40	720	322	1	0	1	737	2.36%	322	0.00%	1	0	1	0.00
75	20	1782	963	3.7	2.7	3.7	1463	-17.89%	789	-18.04%	1.2	0.2	1.2	0.16
75	30	2561	1115	6.8	5	5.6	1993	-22.19%	656	-41.14%	1	0	1	0.14
75	40	1871	716	1.6	0.6	1.6	1759	-5.97%	663	-7.43%	1	0	1	0.12
100	20	3345	1255	8.7	7.3	8.3	2679	-19.92%	837	-33.29%	1	0	1	0.31
100	30	4404	1206	4.8	3.8	4.8	3975	-9.74%	1019	-15.55%	1	0	1	0.16
100	40	4262	1317	3.8	2.8	3.8	3488	-18.18%	1119	-15.05%	1	0	1	0.08
125	20	7327	2302	19.2	18.2	19.2	3935	-46.29%	1146	-50.22%	1	0	1	0.41
125	30	7840	1695	4.1	3.1	4.1	6743	-13.98%	1384	-18.36%	1	0	1	0.04
125	40	8820	1912	6.6	5.4	6.4	7877	-10.69%	1513	-20.88%	1.8	0.5	1.8	19.30

6.2. Case Study of SMOVE

SMOVE, started up in 2012, is one of the one-way carsharing companies in Singapore. It operates Toyota Prius C Hybrid vehicles and has enjoyed fast development over the past few years: the number of stations has grown from 27 stations in 2015 to 49 stations within two years across Singapore. The deployment of those 49 stations is depicted in Figure 6. Users are allowed unlimited mileage and charged according to the hourly packages posted on their website (https://www.smove.sg/). For example, users should pay 50S$ for any rental if its duration is less than 3 hours. In order to implement the proposed model, it is assumed that all the vehicles of SMOVE are EVs and sufficient parking spots equipped with charging facilities are provided in each station. The configuration of those stations, e.g., the driving distance between each station pair is obtained from Google Maps API (Google, 2017). Analogous to the randomly generated instances, the rentals are randomly generated from 7 am to 6 pm with more trips required to depart in the first and last hours.

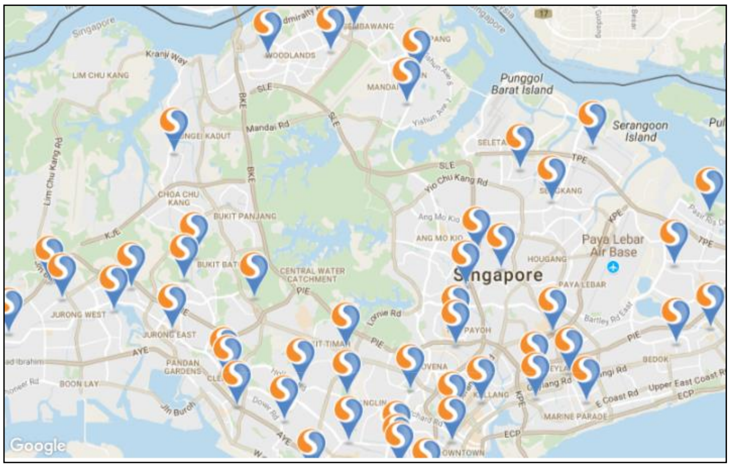

Figure 6. Stations deployment of SMOVE (https://www.smove.sg/)

6.2.1 Assessment of Solution Methods in SMOVE

Ten instances of 150 rentals are generated for the performance comparison of the MILP-reinforced B&P method and the concurrent scheduler based heuristic. The results are reported in Table 4. It shows that the objective value obtained by the concurrent scheduler based heuristic is between 0.09% and 0.43% lower than that by MILP-reinforced B&P approach, however, only a fraction of a second is taken by concurrent scheduler based heuristic. The difference of fleet size is no more than 2. In fact, given a time limit, the solution obtained by the concurrent scheduler based heuristic can be even better than the MILP-reinforced B&P method for larger instances.

To illustrate this, we further generate five instances of 500 rentals to evaluate the two methods within 24 hours, and the results are reported in Table 5. It shows that the MILP-reinforced B&P method cannot solve these instances to optimality within the time limit, and the obtained best solution is far worse than the proposed heuristic in terms of the fleet size and objective value. Moreover, thousands of rentals are generated for the performance evaluation of the concurrent scheduler based heuristic in solving even large-scale problems. The results are shown in Table 6. Hundreds of EVs are required to serve the rentals. As expected, the daily profit of carsharing company increases as the number of rentals grows. It takes no more than 1 minute to obtain the solution of EVFS problem with 5000 rentals.

Table 4. Comparison of MILP-reinforced B&P approach and concurrent scheduler based heuristic on SMOVE with 150 rentals

#Instance	MILP-reinforced B&P			Heuristic				
	FS	Obj (S$)	T_CPU Time (s)	FS	Diff_FS	Obj (S$)	Diff_Obj	T_CPU Time (s)
1	26	10,467	8,961	28	2	10,421	-0.43%	0.22
2	22	10,527	7,791	23	1	10,492	-0.33%	0.13
3	20	10,573	17,543	21	1	10,548	-0.24%	0.12
4	21	10,557	14,658	21	0	10,547	-0.09%	0.13
5	21	10,559	28,550	21	0	10,546	-0.12%	0.13
6	17	10,623	41,085	18	1	10,589	-0.32%	0.07
7	24	10,492	20,638	24	0	10,478	-0.14%	0.14
8	23	10,498	14,930	23	0	10,485	-0.12%	0.11
9	19	10,605	17,430	19	0	10,594	-0.11%	0.11
10	24	10,491	17,314	24	0	10,476	-0.15%	0.16

Table 5. Comparison of MILP-reinforced B&P approach and concurrent scheduler based heuristic on SMOVE with 500 rentals

#Instance	MILP-reinforced B&P			Heuristic				
	FS	Obj (S$)	T_CPU Time (s)	FS	Diff_FS	Obj (S$)	Diff_Obj	T_CPU Time (s)
1	310	30,443	86,400	66	-244	35,273	15.87%	0.51
2	303	30,585	86,400	62	-241	35,364	15.62%	0.75
3	285	30,917	86,400	66	-219	35,292	14.15%	1.09
4	295	30,728	86,400	60	-235	35,423	15.28%	1.03
5	297	30,710	86,400	67	-230	35,296	14.93%	0.90

Table 6. Results of EVFS problem by concurrent scheduler based heuristic on SMOVE with thousands of rentals

#Rental	FS	Profit (S$)	T_CPU Time (s)
1000	122.6	45,766	2.99

2000	222.2	92,101	10.22
3000	339.3	138,050	22.74
4000	443.7	184,320	38.81
5000	561.8	230,330	59.02

6.2.2. Sensitivity Analysis

In light of its great computational efficiency to obtain a good quality solution, we will implement the concurrent scheduler based heuristic in the following sensitivity analysis. Specially, we will explore how the key parameters, i.e., the fixed cost of EV, relocation cost, electricity cost, service charge, EV driving range, the charging efficiency, and the number of rentals, affect the performance of a one-way electric carsharing system. Several performance indicators are reported and they include the optimal EV fleet size (FS), the daily profit of carsharing operator, the number of satisfied rentals (#SR), the satisfied ratio (#SR/#Rental), the usage rate of EV (#SR/FS), the rental duration (RentalTime), the relocation duration (ReloTime), as well as the available time for charging (ChargeTime) approximated by subtracting the sum of rental and relocation duration from the operation period (i.e., 11 hours from 7 am to 6 pm). Unless stated otherwise, the parameter settings are the same with the subsection 6.2.1 except that we randomly generate 10 instances with 500 rentals.

Effect of EV fixed cost

The high capital investment to acquire EV fleets is one of major problems confronted by most carsharing operators. We thus first investigate the effect of fixed cost of EV on the performance of one-way electric carsharing systems. The results are tabulated in Table 7. It shows that the profit of carsharing services will reduce dramatically with the increase of EV cost, demonstrating the dominating influence of EV cost on the profitability of carsharing service[3]. In particular, under the current parameter setting, the carsharing companies will be in the red if the daily EV cost grows beyond 60 S$/veh. Note that not all the rentals are to be satisfied for the profit maximization of the carsharing operator. The increasing EV cost leads to a decreased number of satisfied customers and an increased usage rate, rental and relocation duration of EVs. This suggests that the best strategy of carsharing operators to cope with the rising EV cost is to acquire a smaller fleet of EVs to serve less but the most

[3] The profit in Table 7 can be negative due to the penalty for the denied customers.

profitable customers while increasing the utilization of each vehicle by more frequent vehicle relocations between stations. The available charging time will decrease accordingly.

Table 7. Effect of fixed cost of EV on the performance of an electric carsharing system

EVCost (S$/veh)	FS	Profit (S$)	#SR	#SR/#Rental	#SR/FS	RentalTime (hr/veh)	ReloTime (hr/veh)	ChargeTime (hr/veh)
10	60.2	2,768	497	0.99	8.30	4.81	0.56	5.63
20	55.6	2,076	488	0.98	8.79	5.09	0.85	5.07
30	50.6	1,533	480	0.96	9.48	5.48	1.00	4.52
40	47.9	992	471	0.94	9.83	5.67	1.10	4.23
50	46.4	495	465	0.93	10.03	5.78	1.17	4.04
60	45.4	-3	459	0.92	10.12	5.83	1.24	3.93
70	44.2	-462	454	0.91	10.28	5.90	1.28	3.82
80	41.9	-924	441	0.88	10.52	6.02	1.30	3.68
90	40.5	-1,353	432	0.86	10.66	6.08	1.33	3.59
100	39.1	-1,788	420	0.84	10.75	6.12	1.35	3.53

Effect of variable costs

In addition to the EV fixed cost, we also test the variations of the above performance indicators with respect to the two variable costs, i.e., the relocation cost and the electricity cost, respectively. The results are summarized in Table 8 and Table 9. As expected, they demonstrate the significant effects of relocation and electricity cost on the profitability of carsharing services. In Table 8, higher relocation cost results in less relocation time, while the variation of fleet size is somehow arbitrary. An interesting phenomenon is that the fleet size sometimes decreases simultaneously with reduced vehicle relocation due to the rise of relocation cost. This appears contrary to the acknowledged trade-off effect between fleet size and vehicle relocation. We caution that the trade-off effect may be only valid if all the rentals are required to be served. For the obtained results, we guess that when the relocation cost increases, the operators are suggested to serve less profitable customers who are more conveniently to be served by less vehicle relocation. Table 9 indicates that with the increase of electricity cost, the operators should serve a reduced number of customers by a smaller fleet. The trade-off effect between fleet size and vehicle relocation become visible.

Table 8. Effect of relocation cost on the performance of an electric carsharing system

ReloCost (S$/min)	FS	Profit (S$)	#SR	#SR/#Rental	#SR/FS	RentalTime (hr/veh)	ReloTime (hr/veh)	ChargeTime (hr/veh)
0.3	55.6	2,076	488	0.98	8.79	5.09	0.85	5.07
0.6	55.5	1,923	487	0.97	8.80	5.10	0.82	5.08

0.9	55	1,800	487	0.97	8.87	5.14	0.80	5.06
1.2	53.8	1,679	486	0.97	9.04	5.24	0.78	4.98
1.5	54.5	1,533	486	0.97	8.93	5.18	0.76	5.06
1.8	54.4	1,430	486	0.97	8.95	5.19	0.73	5.08
2.1	54.6	1,307	487	0.97	8.93	5.18	0.72	5.10
2.4	54.3	1,216	487	0.97	8.97	5.20	0.70	5.10
2.7	53.9	1,109	485	0.97	9.01	5.23	0.69	5.08
3	54.3	1,006	486	0.97	8.96	5.20	0.67	5.13

Table 9. Effect of electricity cost on the performance of an electric carsharing system

EleCost (S$/kWh)	FS	Profit (S$)	#SR	#SR/#Rental	#SR/FS	RentalTime (hr/veh)	ReloTime (hr/veh)	ChargeTime (hr/veh)
0.33	56.2	2,172	489	0.98	8.72	5.05	0.84	5.11
0.37	56	2,125	489	0.98	8.75	5.06	0.84	5.10
0.40	55.6	2,076	488	0.98	8.79	5.09	0.85	5.07
0.43	55.9	2,037	489	0.98	8.76	5.07	0.84	5.09
0.47	55.5	1,995	488	0.98	8.82	5.10	0.85	5.05
0.50	54.9	1,942	487	0.97	8.88	5.14	0.85	5.01
0.53	54.8	1,900	487	0.97	8.90	5.15	0.85	5.00
0.57	54.4	1,862	486	0.97	8.95	5.19	0.86	4.96
0.60	54.6	1,806	486	0.97	8.92	5.16	0.86	4.98
0.63	54.3	1,768	486	0.97	8.97	5.19	0.86	4.95

Effect of service charge

We further examine the effect of service charge on the performance of carsharing systems. The results are presented in Table 10. It shows that if the service charge is set to be below 0.1S$/min, the operator would be at a loss. By setting a higher service charge, all the rentals become more profitable than before, and the operators are suggested to serve more customers by a larger EV fleet. Similar to the diminishing return in economics, the utilization rate of EV will decrease with the fleet expansion. The trade-off effect between fleet size and vehicle relocation is obvious under this scenario. We caution that the underlying assumption behind the above results is the in-elasticity of customer demands with respect to service charge. Readers may refer to the studies by Jorge et al. (2015) and Xu et al. (2018) regarding the performance of carsharing systems considering demand elasticity.

Table 10. Effect of service charge on the performance of an electric carsharing system

Charge (S$/min)	FS	Profit (S$)	#SR	#SR/#Rental	#SR/FS	RentalTime (hr/veh)	ReloTime (hr/veh)	ChargeTime (hr/veh)
0.1	41	-345	434	0.87	10.59	6.05	1.28	3.66
0.15	46.7	229	467	0.93	10.00	5.76	1.11	4.13
0.2	48.4	833	473	0.95	9.78	5.65	1.02	4.33

0.25	52.4	1,464	484	0.97	9.24	5.34	0.92	4.74
0.3	55.6	2,073	488	0.98	8.80	5.09	0.85	5.06
0.35	57.2	2,753	491	0.98	8.61	4.99	0.74	5.27
0.4	58.6	3,402	494	0.99	8.46	4.90	0.69	5.41
0.45	60.1	4,069	496	0.99	8.28	4.80	0.63	5.57
0.5	59.5	4,741	497	0.99	8.38	4.85	0.59	5.55
0.55	60	5,394	497	0.99	8.32	4.82	0.57	5.61

Effect of EV battery capacity

As introduced previously, EVs cause additional managerial problems for carsharing operators due to their limited driving range. Since battery capacity is the decisive factor for the driving range of EV, we also explore how the variation of battery capacity affects the performance of an electric carsharing system. The battery capacity ranging from 12 kWh to 66 kWh is considered in the sensitivity analysis, which is correspondent to the driving range of an EV from 68 km to 375 km per charge. As illustrated in Table 11, the increasing of battery capacity leads to an increase of profit by a smaller EV fleet and a higher EV utilization rate. In addition to the reduced cost to acquire EVs, the additional profit should also be attributed to the flexibility the extended driving range offers to the carsharing operator to serve more profitable customer orders which are generally associated with a longer rental duration and probably more electricity consumption. This may partially be verified by the increased rental duration due to the enlarged battery capacity. The relocation time shows a similar increase trend with respect to the enhancement of battery capacity. A larger battery and an extended driving range require less charging time for the operation of carsharing services.

Table 11. Effect of EV battery capacity (i.e., driving range) on the performance of an electric carsharing system

BatteryCap (kWh)	FS	Profit (S$)	#SR	#SR/#Rental	#SR/FS	RentalTime (hr/veh)	ReloTime (hr/veh)	ChargeTime (hr/veh)
12	61	1,818	491	0.98	8.06	4.65	0.64	5.71
18	56.9	1,959	488	0.98	8.60	4.97	0.76	5.27
24	56.9	2,023	489	0.98	8.62	4.99	0.81	5.20
30	55.6	2,076	488	0.98	8.79	5.09	0.85	5.07
36	54.8	2,129	488	0.98	8.91	5.17	0.86	4.97
42	54.3	2,175	489	0.98	9.02	5.23	0.88	4.89
48	53.6	2,212	490	0.98	9.15	5.30	0.89	4.81
54	52.9	2,237	489	0.98	9.26	5.37	0.92	4.71
60	52.5	2,250	489	0.98	9.31	5.41	0.91	4.68

66	52.7	2,256	489	0.98	9.29	5.39	0.93	4.68

Effect of charging efficiency

We further investigate the effect of charging efficiency, measured by the constant charging current I_{cc} in the CC phase, on the performance of electric carsharing systems. According to the battery circuit model in Section 2.3, the entire charging profile will also be adjusted accordingly when we vary the charging current of the CC phase I_{cc}. The variation of the performance indicators with respect to I_{cc} are reported in Table 12. We consider the values of I_{cc} ranging from 12 A to 30 A in the analysis, which are all within the charging efficiency of most real-world normal charging stations. It can be found that the effect of charging efficiency is similar to that of battery capacity. For example, the increase of charging efficiency leads to an increased profit and a decreased fleet size. However, the variation magnitudes of the performance indicators including the profit, fleet size, utilization rate, and time-related parameters are less than those resulted from the variation of battery capacity. This suggests that deploying more efficient charging equipments has similar positive effect on the system performance to acquiring EV with a larger battery capacity. The carsharing operators should balance the cost and benefit when making choice among the two alternatives to enhance their service operation.

Table 12. Effect of I_{cc} (i.e., charging efficiency) on the performance of an electric carsharing system

I_{cc} (A)	FS	Profit (S$)	#SR	#SR/#Rental	#SR/FS	RentalTime (hr/veh)	ReloTime (hr/veh)	ChargeTime (hr/veh)
12	55.6	2,076	488	0.98	8.79	5.09	0.85	5.07
14	55	2,100	489	0.98	8.90	5.16	0.87	4.98
16	53.8	2,122	488	0.98	9.08	5.27	0.88	4.85
18	53.8	2,127	488	0.98	9.08	5.27	0.87	4.86
20	53.7	2,134	488	0.98	9.11	5.28	0.88	4.83
22	53.6	2,144	489	0.98	9.13	5.30	0.88	4.82
24	53.4	2,146	489	0.98	9.17	5.32	0.89	4.79
26	53.5	2,153	489	0.98	9.16	5.31	0.88	4.80
28	53.2	2,153	489	0.98	9.20	5.34	0.89	4.77
30	53.4	2,154	489	0.98	9.17	5.32	0.89	4.79

Effect of rental number

Last, we investigate the variations of these performance indicators with respect to the growth of user demands and the results are shown in Table 13. We can see from the results that with the increasing number of rentals, the operators can earn more profit by serving more and the most profitable rentals with a larger fleet of EVs. Both the satisfied ratio and the usage rate of EV show a visible increase trend along with the growth of user demands. This means that with the increasing popularity of carsharing services among customers, the operators could improve the overall utilization of EV fleets while achieving a higher level of service. Regarding the time allocation of EVs, the results indicate that more time will be used to serve the customers and less relocation is needed which may be attributed to the self-vehicle-rebalance due to the increasing number of users.

Table 13. Effect of rental number on the performance of an electric carsharing system

#Rental	FS	Profit (S$)	#SR	#SR/#Rental	#SR/FS	RentalTime (hr/veh)	ReloTime (hr/veh)	ChargeTime (hr/veh)
100	13.9	357	97	0.97	7.05	4.16	1.02	5.81
200	23.5	788	194	0.97	8.28	4.85	1.03	5.12
300	36.2	1,176	292	0.97	8.13	4.73	0.92	5.35
400	46.4	1,670	392	0.98	8.50	4.96	0.86	5.17
500	58	2,081	490	0.98	8.49	4.96	0.83	5.22
600	68.5	2,523	590	0.98	8.62	4.98	0.77	5.26
700	79.5	2,924	686	0.98	8.66	5.00	0.78	5.22
800	89.5	3,425	784	0.98	8.79	5.11	0.72	5.17
900	100.6	3,843	882	0.98	8.78	5.08	0.67	5.25
1000	109.4	4,449	986	0.99	9.04	5.24	0.62	5.14

7. Conclusions

This study investigated the EVFS problem for the one-way carsharing services by taking into account the necessary practical requirement of vehicle relocation operations and nonlinear EV charging profile. Based on the set partitioning model built for the considered EVFS problem, a tailored B&P approach was developed to find a global optimal solution. The multi-label method incorporating the non-dominated charging strategy was developed to solve the essential pricing problem. We further designed two heuristic methods, i.e., the concurrent scheduler based heuristic and a MILP-based heuristic method, for solving the large-scale problems and reinforcing the B&P approach respectively. These solution methods were compared and evaluated by numerical experiments and the results have demonstrated their competence under different problem settings.

This study was made based on the assumption that the information of rentals is known a priori by estimation/prediction. For practical applications of the proposed approach, these demand information may be obtained by market survey. The respondents might be asked about their preference for the carsharing service, especially the most possible origin and destination as well as the starting and end times of carsharing trips. The collected demand information will then be used as the input for the proposed model and method to determine the fleet size for the carsharing services. The result serves as a good reference for carsharing operators if the estimated demand is not largely deviated from the real demand. Moreover, the proposed method can also be used in “offline” EV sharing applications such as dial-and-ride problems or reservation-based carsharing systems.

For the one-way carsharing services with EVs, it would be interesting to consider charging en route and time window of rentals in the future. Due to complexity of the considered problem, the current study assumed uncapacitated charging facilities. Relaxation of this assumption without adding too much complexity to the model and solution method is one of future research challenges. Most of the existing carsharing systems are subject to significant stochasticity and uncertainties in both the demand and the operating parameters (e.g., rental duration, electricity consumption, driving range of EVs, etc.). Incorporating the uncertainties of those factors would make the study more align with reality. Customized approaches involving robust optimization and stochastic programming might be helpful. Combining the elastic demand with the flexible destination choice of users may be practically relevant, because many carsharing companies allow users to change their destinations during the rental period. Last but not the least, in addition to the tactical decision-making for the carsharing services, it is of great significance for the carsharing operators to develop an online decision platform for the operational level decision-makings such as vehicle relocation, dynamic trip pricing, charging strategy, and/or personnel assignment. In particular, the current study does not consider the impact of the charging strategy on the battery health in a long term. It is often suggested in the practice to initiate the charging of fleet vehicles as closely as possible to the departure time because the battery ages faster when stored at a higher SOC. An operational charging strategy concerning the time clock to initiate charging and the charging duration may be investigated in the future when the main concern is to propose a specific charging strategy for the sake of battery health as well as the profitability of carsharing service.

References

Adler, J. D., Mirchandani, P. B., 2016. The vehicle scheduling problem for fleets with alternative-fuel vehicles. *Transportation Science, 51*(2), 441-456.

Andelmin, J., Bartolini, E., 2017. An exact algorithm for the green vehicle routing problem. *Transportation Science*, *51*(4), 1288-1303.

Ball, M., 1980. A comparison of relaxations and heuristics for certain crew and vehicle scheduling problems. In *National ORSA/TIMS Meeting, Washington, DC*.

Barnhart, C., Johnson, E. L., Nemhauser, G. L., Savelsbergh, M. W., Vance, P. H., 1998. Branch-and-price: Column generation for solving huge integer programs. *Operations Research*, *46*(3), 316-329.

Ben Amor, H., Desrosiers, J., Valério de Carvalho, J. M., 2006. Dual-optimal inequalities for stabilized column generation. *Operations Research, 54*(3), 454-463.

Benjaafar, S., Li, X., Li, X., 2017. Inventory repositioning in on-demand product rental networks. *Working Paper*.

Bodin, L., Rosenfield, D., Kydes, A., 1978. UCOST: a micro approach to a transportation planning problem. *Journal of Urban Analysis*, *5*(1), 47-69.

Boyacı, B., Zografos, K.G., Geroliminis, N., 2015. An optimization framework for the development of efficient one-way car-sharing systems. *European Journal of Operational Research*, *240*(3), 718-733.

Boyacı, B., Zografos, K. G., Geroliminis, N., 2017. An integrated optimization-simulation framework for vehicle and personnel relocations of electric carsharing systems with reservations. *Transportation Research Part B: Methodological*, *95*, 214-237.

Boysen, N., Briskorn, D., Emde, S., 2018. Scheduling electric vehicles and locating charging stations on a path. *Journal of Scheduling*, *21*(1), 111-126.

Brandstätter, G., Gambella, C., Leitner, M., Malaguti, E., Masini, F., Puchinger, J., Ruthmair M., Vigo, D., 2016. Overview of optimization problems in electric car-sharing system design and management. In *Dynamic Perspectives on Managerial Decision Making* (pp. 441-471). Springer, Cham.

Brandstätter, G., Kahr, M., Leitner, M., 2017. Determining optimal locations for charging stations of electric car-sharing systems under stochastic demand. *Transportation Research Part B: Methodological*, *104*, 17–35.

Bruglieri, M., Colorni, A., Luè, A., 2014. The relocation problem for the one-way electric vehicle sharing. *Networks*, *64*(4), 292-305.

Bruglieri, M., Pezzella, F., Pisacane, O., 2017. Heuristic algorithms for the operator-based relocation problem in one-way electric carsharing systems. *Discrete Optimization*, *23*, 56-80.

Chang, J., Yu, M., Shen, S., Xu, M., 2017. Location Design and Relocation of a Mixed Car-Sharing Fleet with a CO_2 Emission Constraint. *Service Science*, 9(3), 205-218.

Desaulniers, G., Errico, F., Irnich, S., Schneider, M., 2016. Exact algorithms for electric vehicle-routing problems with time windows. *Operations Research*, *64*(6), 1388-1405.

Desrochers, M., Soumis, F., 1989. A column generation approach to the urban transit crew scheduling problem. *Transportation Science*, *23*(1), 1-13.

Erdoğan, S., Miller-Hooks, E., 2012. A green vehicle routing problem. *Transportation Research Part E: Logistics and Transportation Review*, *48*(1), 100-114.

Google, 2017. Google Maps API. https://developers.google.com/maps/ (accessed 17/10/2018).

He, L., Hu, Z., Zhang, M., 2018. Robust repositioning for vehicle sharing. *Manufacturing & Service Operations Management*, Forthcoming.

He, L., Mak, H. Y., Rong, Y., Shen, Z. J. M., 2017. Service region design for urban electric vehicle sharing systems. *Manufacturing & Service Operations Management*, 19(2), 309-327.

Hiermann, G., Puchinger, J., Ropke, S., Hartl, R. F., 2016. The electric fleet size and mix vehicle routing problem with time windows and recharging stations. *European Journal of Operational Research*, *252*(3), 995-1018.

Illgen, S., Höck, M., 2018. Electric vehicles in car sharing networks–Challenges and simulation model analysis. *Transportation Research Part D: Transport and Environment*, *63*, 377-387.

Irnich, S., Desaulniers, G., 2005. Shortest path problems with resource constraints. In *Column Generation* (pp. 33-65). Springer, Boston, MA.

Jorge, D., Molnar, G., de Almeida Correia, G. H., 2015. Trip pricing of one-way station-based carsharing networks with zone and time of day price variations. *Transportation Research Part B: Methodological*, *81*, 461-482.

LTA (Land Transport Authority), 2014. Joint news release by the land transport authority & EDB on EV phase 2 – share an electric car. http://www.lta.gov.sg/apps/news/page.aspx?c=2&id=b1f98bcd-e4fc-4902-9f9d-08bc2309c3df (accessed 17/10/2018).

Laporte, G., Pascoal, M. M., 2011. Minimum cost path problems with relays. *Computers & Operations Research*, *38*(1), 165-173.

Larminie, J., Lowry, J., 2012. *Electric vehicle technology explained*. John Wiley & Sons.

Li, X., Ma, J., Cui, J., Ghiasi, A., Zhou, F., 2016. Design framework of large-scale one-way electric vehicle sharing systems: A continuum approximation model. *Transportation Research Part B: Methodological*, *88*, 21-45.

Liu, W., 2013. *Introduction to hybrid vehicle system modeling and control*. John Wiley & Sons.

Lu, M., Chen, Z., Shen, S., 2017. Optimizing the profitability and quality of service in carshare systems under demand uncertainty. *Manufacturing & Service Operations Management*, 20(2), 162-180.

Madankumar, S., Rajendran, C., 2018. Mathematical models for green vehicle routing problems with pickup and delivery: A case of semiconductor supply chain. *Computers & Operations Research*, *89*, 183-192.

Marra, F., Yang, G. Y., Træholt, C., Larsen, E., Rasmussen, C. N., You, S., 2012. Demand profile study of battery electric vehicle under different charging options. In *Power and Energy Society General Meeting, 2012 IEEE* (pp. 1-7). IEEE.

Montoya, A., Guéret, C., Mendoza, J. E., Villegas, J. G., 2017. The electric vehicle routing problem with nonlinear charging function. *Transportation Research Part B: Methodological*, *103*, 87-110.

Nissan, 2018. Nissan Leaf. http://www.nissanusa.com/electric-cars/leaf/ (accessed 17/10/2018).

Nourinejad, M., Roorda, M. J., 2014. A dynamic carsharing decision support system. *Transportation research part E: logistics and transportation review*, *66*, 36-50.

Nourinejad, M., Zhu, S., Bahrami, S., Roorda, M. J., 2015. Vehicle relocation and staff rebalancing in one-way carsharing systems. *Transportation Research Part E: Logistics and Transportation Review*, *81*, 98-113.

Pelletier, S., Jabali, O., Laporte, G., 2016. 50th anniversary invited article—goods distribution with electric vehicles: review and research perspectives. *Transportation Science*, *50*(1), 3-22.

Pelletier, S., Jabali, O., Laporte, G., Veneroni, M., 2017. Battery degradation and behaviour for electric vehicles: Review and numerical analyses of several models. *Transportation Research Part B: Methodological*, *103*, 158-187.

Ryan, D. M., Foster, B. A., 1981. An integer programming approach to scheduling. *Computer scheduling of public transport urban passenger vehicle and crew scheduling*, A. Wren (ed.), North-Holland, Amsterdam, 269-280.

Schneider, M., Stenger, A., Goeke, D., 2014. The electric vehicle-routing problem with time windows and recharging stations. *Transportation Science*, *48*(4), 500-520.

Shaheen, S., Cohen, A., 2012. Innovative mobility carsharing outlook: carsharing market overview, analysis, and trends: fall 2012. Transportation Sustainability Research Center, Institute of Transportation Studies. *University of California, Berkeley*.

Sweda, T. M., Dolinskaya, I. S., Klabjan, D., 2017. Adaptive routing and recharging policies for electric vehicles. *Transportation Science*, *51*(4), 1326-1348.

Taxi, 2018. Taxi Singapore. http://www.taxisingapore.com/taxi-fare/ (accessed 17/10/2018).

Toth, P., Vigo, D. (Eds.), 2002. *The vehicle routing problem*. Society for Industrial and Applied Mathematics.

Weikl, S., Bogenberger, K., 2015. A practice-ready relocation model for free-floating carsharing systems with electric vehicles–Mesoscopic approach and field trial results. *Transportation Research Part C: Emerging Technologies*, *57*, 206-223.

Xu, M., Meng, Q., Liu, Z., 2018. Electric vehicle fleet size and trip pricing for one-way carsharing services considering vehicle relocation and personnel assignment. *Transportation Research Part B: Methodological*, *111*, 60-82.

Zhao, M., Li, X., Yin, J., Cui, J., Yang, L., An, S., 2018. An integrated framework for electric vehicle rebalancing and staff relocation in one-way carsharing systems: Model formulation and Lagrangian relaxation-based solution approach. *Transportation Research Part B: Methodological*, *117*, 542-572.

Appendix: Notations

i	Index for rental
$\mathcal{I}$	Set of rentals
s	Index for station
$\mathcal{S}$	Set of stations
r	Index for trip chain
$\mathcal{R}$	Set of feasible trip chains
$\bar{\mathcal{R}}$	Subset of columns/feasible trip chains
n_r	Number of rentals in trip chain r
k, j	Index for subscript of a rental in a trip chain
s_i^o	Pick-up station of rental i
s_i^d	Drop-off station of rental i
t_i^o	Departure time of rental i
t_i^d	Arrival time of rental i

e_i	Electricity consumption of rental i
G_i	Revenue collected from rental i
OC_i	Operating cost incurred by rental $i \in \mathcal{I}$,
RC_{ij}	Relocation cost from the drop-off station of rental $i \in \mathcal{I}$ to the pick-up station of rental $j \in \mathcal{I}$
EC	Fixed operational cost of an EV measured in \$/veh-day
P_i	Penalty for rejecting rental i
$\tau(s_i^d, s_j^o)$	Travel time on the shortest path from the drop-off station of rental $i \in \mathcal{I}$ to the pick-up station of rental $j \in \mathcal{I} \setminus \{i\}$
$e(s_i^d, s_j^o)$	Electricity consumption on the shortest path from the drop-off station of rental $i \in \mathcal{I}$ to the pick-up station of rental $j \in \mathcal{I} \setminus \{i\}$
$w(s_i^o)$	Amount of electricity charged at the pick-up station (s_i^o) of rental i
$\tau(s_i^o)$	Charging duration at the pick-up station (s_i^o) of rental i
$w(s_i^d)$	Amount of electricity charged at the drop-off station (s_i^d) of rental i
$\tau(s_i^d)$	Charging duration at the drop-off station (s_i^d) of rental i
SOC_{init}	Initial SOC of an EV at the very beginning of operation period.
SOC_{i_j}	SOC at the end of rental i_j , $j = 1, 2, ..., n_r$
$SOC_{i_j, i_{j+1}}$	SOC right at the end of relocation between the drop-off station of rental i_j and pick-up station of rental i_{j+1} , $j = 1, 2, ..., n_r - 1$
SOC_{comf}	Minimal SOC value that frees drivers from range anxiety
R_r	Revenue of trip chain r
E_r	Variable cost of trip chain r
SOC_0	Initial SOC before charging
I_{CC}	Constant charging current at the CC phase
Cap	Maximum possible charge the battery can hold
$\hat{t}$	Switch time point from CC phase to CV phase
$S\hat{O}C$	Maximum SOC achieved at the end of CC phase
SOC_{max}	Maximum SOC achievable at the end of CV phase
T_{max}	Duration of CV phase
SOC_{cutoff}	Cut-off SOC value to avoid over-discharging.
$f(\cdot)$	Function of SOC with respect to time duartion t starting at time clock $\hat{t}$ when entering CV phase
$f^{-1}(\cdot)$	Inverse function of $f(t)$
δ_r^i	Binary coefficient which equal 1 is rental i is covered by trip chain r , and 0 otherwise

x_r	Binary decision variable and $x_r = 1$ if trip chain $r \in \mathcal{R}$ is performed by an EV in the fleet.
π_i	Dual value of each constraint (excluding the non-negativity constraints) in the model [EVFS-MP]
$\mathcal{G} = (\mathcal{I}, \mathcal{A})$	Constructed pseudo-network for pricing problem
c_i	Cost of node $i \in \mathcal{I}$ in the pseudo-network $\mathcal{G}$
c_{ij}	Cost of link $ij \in \mathcal{A}$ in the pseudo-network $\mathcal{G}$
m_{ij}	Charging strategy for link ij
m_{ij}^*	Non-dominated charging strategy for link ij
M_{ij}	Set of all the feasible charging strategies for link ij
$SOC_j^o(SOC_i, m_{ij})$	SOC at the departure time clock of rental j after setting off from the drop-off station of rental i with SOC at SOC_i and being charged by any charging strategy m_{ij}
q_r	Charging strategy for trip chain r
q_r^*	Non-dominated charging strategy for trip chain r
Q_r	Set of all the feasible charging strategies for trip chain r
$SOC_{i_k}^o(SOC_{init}, n_r)$	SOC at the departure time clock of rental i_k of trip chain $r = s_{i_1}^o \to s_{i_1}^d \Rightarrow s_{i_2}^o \to s_{i_2}^d \Rightarrow \cdots \Rightarrow s_{i_{n_r}}^o \to s_{i_{n_r}}^d$ after setting off from the pick-up station of rental i_1 with SOC at SOC_{init} and being charged by any charging strategy n_r
$l_k(i)$	Label k at node i, $l_k(i) \triangleq [\hat{c}_k, \hat{w}_k, \gamma_k, \kappa_k]$, where $\hat{c}_k$ and $\hat{w}_k$ are the profit, i.e., minus of the cost, and current value of SOC of path k ending at the drop-off station of node/rental i, respectively; γ_k and κ_k are the node and label index that precede path k
$\mathcal{L}(i)$	Set of all the labels at node i
$LpObj$	Optimal objective value of the RMP
M	Pre-specified parameter to help fix the long tail effect of column generation
ε_1	Pre-specified tolerance for column generation
P^*	Largest reduced cost, i.e., Optimal objective value of the pricing problem
$\mathcal{R}(i, j)$	Set of trip chains covering both the rental i and rental j
$\mathcal{SI}$	Set of satisfied rentals
$\mathcal{RI}$	Set of rejected rentals
$\mathcal{Q}(i, j)$	Set of trip chains covering the rental i and rental j successively
$\mathcal{IP}$	Set of included pairs of rentals
$\mathcal{EP}$	Set of excluded pairs of rentals

ε_2	Pre-specified tolerance for branch and bound
v	Index for an existing EV/partial trip chain
$\mathcal{V}$	Set of existing EVs/partial trip chains
v_{new}	Index for a new EV
i_v	Index for the last rental of the partial trip chain/EV v
SOC_v	SOC after arriving at the drop-off station of rental i_v
$PROFIT_v^{incumbent}$	Incumbent profit of the partial trip chain/EV v
$PROFIT_v^{incremental}$	Incremental profit for assigning an additional rental after the last rental i_v of the trip chain/EV v